

Higgs Boson Masses in the Complex NMSSM at One-Loop Level

T. Graf*, R. Gröber^a, M. Mühlleitner^a, H. Rzehak^{†b} and K. Walz^a

^a*Institut für Theoretische Physik, Karlsruhe Institute of Technology, 76128 Karlsruhe, Germany*

^b*CERN, PH-TH, 1211 Geneva 23, Switzerland*

Abstract

The Next-to-Minimal Supersymmetric Extension of the Standard Model (NMSSM) with a Higgs sector containing five neutral and two charged Higgs bosons allows for a rich phenomenology. In addition, the plethora of parameters provides many sources of CP violation. In contrast to the Minimal Supersymmetric Extension, CP violation in the Higgs sector is already possible at tree-level. For a reliable understanding and interpretation of the experimental results of the Higgs boson search, and for a proper distinction of Higgs sectors provided by the Standard Model or possible extensions, the Higgs boson masses have to be known as precisely as possible including higher-order corrections. In this paper we calculate the one-loop corrections to the neutral Higgs boson masses in the complex NMSSM in a Feynman diagrammatic approach adopting a mixed renormalization scheme based on on-shell and $\overline{\text{DR}}$ conditions. We study various scenarios where we allow for tree-level CP-violating phases in the Higgs sector and where we also study radiatively induced CP violation due to a non-vanishing phase of the trilinear coupling A_t in the stop sector. The effects on the Higgs boson phenomenology are found to be significant. We furthermore estimate the theoretical error due to unknown higher-order corrections by both varying the renormalization scheme of the top and bottom quark masses and by adopting different renormalization scales. The residual theoretical error can be estimated to about 10%.

*Present email address: thorben_graf@gmx.de

†On leave from: Albert-Ludwigs-Universität Freiburg, Physikalisches Institut, Freiburg, Germany.

1 Introduction

The search for the Higgs boson and ultimately the understanding of the mechanism behind the creation of particle masses represents one of the major goals of the Large Hadron Collider (LHC). Recently, the experimental collaborations ATLAS and CMS have updated their results on the search for the Higgs boson. Both experiments observe an excess of events in the low Higgs mass range, compatible with a Standard Model (SM) Higgs boson mass hypothesis close to 124 GeV at 3.1σ local significance as reported by CMS [1] and close to 126 GeV at 3.5σ local significance in the ATLAS experiment [2]. This is still too far away from the 5σ required to claim discovery and necessitates the accumulation of further data in the ongoing experiment. The slight excess of events in the $\gamma\gamma$ final state signature as compared to the Standard Model expectation may hint to the existence of new physics. One of the most popular extensions of the SM are supersymmetric models (SUSY) [3]. While the Higgs sector of the Minimal Supersymmetric Extension (MSSM) [4] consists of two complex Higgs doublets, which lead to five physical Higgs states after electroweak symmetry breaking (EWSB), the Next-to-Minimal Supersymmetric Model (NMSSM) [5] extends the Higgs sector by an additional singlet superfield \hat{S} . This entails 7 Higgs bosons after EWSB, which in the limit of the real NMSSM can be divided into three neutral purely CP-even, two neutral purely CP-odd and two charged Higgs bosons, and in total leads to five neutralinos. Although more complicated than the MSSM, the NMSSM has several attractive features. Thus it allows for the dynamical solution of the μ problem [6] through the scalar component of the singlet field acquiring a non-vanishing vacuum expectation value. Furthermore, the tree-level mass value of the lightest Higgs boson is increased by new contributions to the quartic coupling so that the radiative corrections necessary to shift the Higgs mass to ~ 125 GeV are less important than in the MSSM allowing for lighter stop masses¹ and less finetuning [7–9]. The enlarged Higgs and neutralino sectors, finally, lead to a richer phenomenology both in collider and dark matter (DM) experiments. The latter is due to the possibility of a singlino-like lightest neutralino, the former due to heavier Higgs bosons decaying into lighter ones at sizeable rates or due to possibly enhanced or suppressed branching ratios in LHC standard search channels such as $\gamma\gamma$ or vector boson final states [9, 10], to cite only a few of the possible modifications compared to SM or MSSM phenomenology.

The enlarged parameter set in supersymmetric theories allows for further sources of CP violation as compared to the SM, where the only source of CP violation occurs in the CKM matrix. Hence, the soft SUSY breaking couplings and gaugino masses as well as the Higgsino mixing parameter μ can be complex. While in the MSSM CP violation in the Higgs sector is not possible at tree-level due to the minimality conditions of the Higgs potential, it can be radiatively induced through non-vanishing CP phases [11–13]. Consequently, the CP-even and CP-odd Higgs bosons mix so that the physical states have no definite CP quantum number any more leading to substantial modifications in Higgs boson phenomenology [14]. The Higgs couplings to the SM gauge bosons and fermions, their SUSY partners and the Higgs self-couplings can be considerably modified compared to the CP-conserving case inducing significant changes in the Higgs boson production rates and decay modes. This could allow for Higgs bosons with masses below present exclusion bounds from LEP and possibly Tevatron and LHC as they might have escaped detection due to suppressed couplings involved in the various standard Higgs search channels, which would then necessitate new search

¹The bulk of the radiative corrections stems from the (s)top loops.

strategies [15].

In the NMSSM CP violation in the Higgs sector is possible at tree-level. Though spontaneous tree-level CP violation in the Z_3 -invariant NMSSM is impossible due to vacuum stability [16], explicit CP violation can be realized already at tree-level in contrast to the MSSM. In principle, there can be six complex phases parametrizing the CP violation in the Higgs sector, two relative phases between the vacuum expectation values (VEVs) of the Higgs doublet and singlet fields and four phases for the complex parameters $\lambda, \kappa, A_\lambda, A_\kappa$. At tree-level these phases appear only in certain combinations, however, and exploiting tadpole conditions we are left with only one independent phase combination. Explicit CP violation in the Higgs sector leads to potentially large corrections to the electric dipole moments (EDMs). The non-observation of EDMs for thallium, neutron and mercury [17] severely constrains the CP-violating phases. However, as the phase combinations occurring in the EDMs can be different from the ones inducing Higgs mixing, the phases can be chosen such that the contributions to the EDMs are small while the phases important for the Higgs sector can still be sizeable [18]. This provides additional CP violation necessary for electroweak baryogenesis [19]. The explicit tree-level CP violation induces scalar-pseudoscalar mixings between the doublet fields $H_{u,d}$ and the singlet field S , but not between the scalar and pseudoscalar components of the Higgs doublets $H_{u,d}$. The latter is realized in scenarios where explicit CP violation in the Higgs sector is induced through radiative corrections. Radiative CP violation furthermore allows for a moderate amount of CP violation which is still in agreement with the bounds from the EDMs [20]. In this respect, the CP phases which play a role are $\varphi_{A_t}, \varphi_{A_b}$ from the trilinear couplings A_t, A_b . They are involved in the dominant corrections from the third generation squark loops. Phases from third generation Yukawa couplings on the other hand can be reabsorbed by redefinitions of the quark fields when neglecting generation mixing. Further sources for radiative CP violation stem from the gaugino sector where the soft SUSY breaking mass parameters M_1, M_2 and M_3 are in general complex. One of the two parameters M_1 and M_2 can be chosen real by applying an R -symmetry transformation. The gluino mass parameter M_3 and hence its phase enters only at the two-loop level.

Radiatively induced CP-violating effects from the third generation squark sector have been considered in the effective potential approach at one-loop level in Refs. [21]. One-loop contributions from the charged particle loops have been taken into account by Refs. [22], also in the effective potential approach. In Ref. [23] the third generation (s)quark and gauge contributions are included in the one-loop effective potential. The full one-loop and logarithmically enhanced two-loop effects in the renormalization-group improved approach have been included in [24]. In order to properly interpret the results from the experiments and distinguish the various Higgs sectors from each other, a precise knowledge of the Higgs boson masses and couplings at the highest possible accuracy, including higher-order corrections, is indispensable. In this paper we consider the full one-loop corrections to the Higgs boson masses in the CP-violating NMSSM in the Feynman diagrammatic approach.² We allow for explicit CP violation at tree-level by including non-vanishing CP phases for the Higgs doublets and singlet, as well as for $\lambda, \kappa, A_\lambda$ and A_κ , which effectively reduce to one physical CP phase combination at tree-level when the tadpole conditions are exploited. We

²Higher-order corrections to the Higgs boson masses in the real NMSSM can be found in Refs. [25, 26].

furthermore allow for radiatively induced CP violation stemming from the stop³ by choosing a non-vanishing CP phase for A_t . The Higgs sector as well as the neutralino and chargino sector will be used to determine the counterterms. The renormalization is performed in a mixed scheme which combines $\overline{\text{DR}}$ conditions for the parameters not directly related to physical observables with on-shell (OS) conditions for the physical input values. For the choice of our parameter sets the recent constraints from the Higgs boson searches at LEP [27], Tevatron [28] and LHC [1, 2] are taken into account. The inclusion of CP violation affects the Higgs phenomenology and hence the validity of possible scenarios. Our results will therefore help to clarify the question what kind of Higgs sector may be realized in nature for a SM-like Higgs boson with mass around 125 GeV, should the tantalizing hints of the LHC experiments be confirmed by the discovery of the Higgs boson at the 5σ level once a sufficient amount of data is accumulated.

The organization of the paper is as follows. In Sect. 2 the parameters of the complex NMSSM will be introduced. Section 3 presents the details of our calculation. After introduction of the complex tree-level Higgs sector in Sect. 3.1 the set of input parameters is given in Sect. 3.2. The renormalization conditions and determination of the Higgs masses as well as the mixing angles are discussed in Sects. 3.3 and 3.4, respectively. In Sect. 4 we present our numerical analysis, discuss the influence of different renormalization schemes as well as the consequences of one-loop corrections in the complex NMSSM for the Higgs boson phenomenology and results at the LHC. We terminate with the conclusions in Sect. 5.

2 Complex parameters in the NMSSM

The Lagrangian of the complex NMSSM can be divided into an MSSM part which is adopted from the MSSM Lagrangian and an additional NMSSM part. The latter contains (apart from the phases of the Higgs doublets and singlets) four additional complex parameters. Two of them are the coupling κ of the self-interaction of the new singlet superfield \hat{S} and the coupling λ for the interaction of \hat{S} with the Higgs doublet superfields \hat{H}_u and \hat{H}_d (\hat{H}_u and \hat{H}_d couple to the up- and down-type quark superfields, respectively). They are introduced via the extension of the MSSM superpotential W_{MSSM} ,

$$W_{\text{NMSSM}} = W_{\text{MSSM}} - \epsilon_{ab} \lambda \hat{S} \hat{H}_d^a \hat{H}_u^b + \frac{1}{3} \kappa \hat{S}^3, \quad (1)$$

with $\epsilon_{12} = \epsilon^{12} = 1$. The MSSM part of the superpotential is given by

$$W_{\text{MSSM}} = -\epsilon_{ab} (y_u \hat{H}_u^a \hat{Q}^b \hat{U}^c - y_d \hat{H}_d^a \hat{Q}^b \hat{D}^c - y_e \hat{H}_d^a \hat{L}^b \hat{E}^c), \quad (2)$$

where \hat{Q} and \hat{L} are the left-handed quark and lepton superfield doublets and \hat{U} , \hat{D} and \hat{E} are the right-handed up-type, down-type and electron-type superfield singlets, respectively. The superscript c denotes charge conjugation. Colour and generation indices have been omitted. The quark and lepton Yukawa couplings are given by y_d , y_u and y_e . They are in general complex. However, when neglecting generation mixing, as we assume in this paper, the phases of the Yukawa couplings can be reabsorbed by redefining the quark fields *i.e.* these phases can be chosen arbitrarily without changing the physical meaning [29].

³For the low values of $\tan\beta$ applied in our numerical analysis, the CP-violating effects from the sbottom sector are marginal.

The soft SUSY breaking Lagrangian in the NMSSM is also extended with respect to the MSSM,

$$\mathcal{L}_{\text{NMSSM}}^{\text{soft}} = \mathcal{L}_{\text{MSSM}}^{\text{soft}} - m_S^2 |S|^2 + (\epsilon_{ab} A_\lambda \lambda S H_d^a H_u^b - \frac{1}{3} A_\kappa \kappa S^3 + h.c.), \quad (3)$$

containing two further complex parameters specific to the NMSSM, the soft SUSY breaking trilinear couplings A_λ and A_κ . The MSSM part is given by⁴

$$\begin{aligned} \mathcal{L}_{\text{MSSM}}^{\text{soft}} = & -m_{H_d}^2 |H_d|^2 - m_{H_u}^2 |H_u|^2 - m_Q^2 |\tilde{Q}|^2 - m_U^2 |\tilde{u}_R|^2 - m_D^2 |\tilde{d}_R|^2 - m_L^2 |\tilde{L}|^2 - m_E^2 |\tilde{e}_R|^2 \\ & + \epsilon_{ab} (y_u A_u H_u^a \tilde{Q}^b \tilde{u}_R^* - y_d A_d H_d^a \tilde{Q}^b \tilde{d}_R^* - y_e A_e H_d^a \tilde{Q}^b \tilde{e}_R^* + h.c.) \\ & - \frac{1}{2} (M_1 \tilde{B} \tilde{B} + M_2 \tilde{W}_i \tilde{W}_i + M_3 \tilde{G} \tilde{G} + h.c.). \end{aligned} \quad (4)$$

The soft SUSY breaking trilinear couplings A_u , A_d , A_e of the up-type, down-type and charged lepton-type sfermions⁵, respectively, which are already present in the MSSM, are in general complex. However, the soft SUSY breaking mass parameters of the scalar fields, m_X^2 ($X = S, H_d, H_u, Q, U, D, L, E$), are real. The SM-type and SUSY fields forming a superfield (denoted with a hat) are represented by a letter without and with a tilde, respectively: \tilde{Q} , \tilde{L} and \tilde{u}_R , \tilde{d}_R , \tilde{e}_R are the superpartner fields corresponding to the left- and right-handed quark and lepton fields. In general, also the soft SUSY breaking mass parameters of the gauginos, M_1 , M_2 and M_3 , are complex where the gaugino fields are denoted by \tilde{B} , \tilde{W}_i ($i = 1, 2, 3$) and \tilde{G} for the bino, the winos and the gluinos corresponding to the weak hypercharge $U(1)$, the weak isospin $SU(2)$ and the colour $SU(3)$ symmetry. The R -symmetry can then be exploited to choose either M_1 or M_2 to be real. The kinetic and gauge interaction part of the NMSSM Lagrangian finally do not contain any complex parameters.

Expressing the Higgs boson fields as an expansion about the vacuum expectation values, two further phases appear,

$$H_d = \begin{pmatrix} \frac{1}{\sqrt{2}}(v_d + h_d + ia_d) \\ h_d^- \end{pmatrix}, \quad H_u = e^{i\varphi_u} \begin{pmatrix} h_u^+ \\ \frac{1}{\sqrt{2}}(v_u + h_u + ia_u) \end{pmatrix}, \quad S = \frac{e^{i\varphi_s}}{\sqrt{2}}(v_s + h_s + ia_s). \quad (5)$$

The phases φ_u and φ_s describe the phase differences between the three vacuum expectation values $\langle H_d^0 \rangle$, $\langle H_u^0 \rangle$ and $\langle S \rangle$. In case of vanishing phases, $\varphi_u = \varphi_s = 0$, the fields h_i and a_i with $i = d, u, s$ correspond to the CP-even and CP-odd part of the neutral entries of H_u , H_d and S . The charged components are denoted by h_i^\pm ($i = d, u$).

Exploiting that the phases of the Yukawa couplings can be chosen arbitrarily, the phase of the up-type coupling is set to $\varphi_{y_u} = -\varphi_u$ while the down-type and the charged lepton-type ones are assumed to be real. This choice ensures that the quark and lepton mass terms yield real masses without any further phase transformation of the corresponding fields.

In the following renormalization procedure we will make use of the chargino and neutralino sectors, therefore they are introduced briefly here. The fermionic superpartners of the neutral Higgs

⁴Here the indices of the soft SUSY breaking masses, Q (L) stand for the left-handed doublet of the three quark (lepton) generations and U, D, E are the indices for the right-handed up-type and down-type fermions and charged leptons, respectively. In the trilinear coupling parameters the indices u, d, e represent the up-type and down-type fermions and charged leptons.

⁵We neglect generation mixings so that we have nine complex numbers A_u , A_d , A_e instead of three complex 3×3 matrices.

bosons and colourless gauge bosons are \tilde{H}_d^0 and \tilde{H}_u^0 for the neutral components of the Higgs doublets, \tilde{S} for the Higgs singlet, the bino \tilde{B} and the neutral component \tilde{W}_3 of the winos. After electroweak symmetry breaking these fields mix, and in the Weyl spinor basis $\psi^0 = (\tilde{B}, \tilde{W}_3, \tilde{H}_d^0, \tilde{H}_u^0, \tilde{S})^T$ the neutralino mass matrix M_N can be written as

$$M_N = \begin{pmatrix} M_1 & 0 & -c_\beta M_Z s_{\theta_W} & M_Z s_\beta s_{\theta_W} e^{-i\varphi_u} & 0 \\ 0 & M_2 & c_\beta M_W & -M_W s_\beta e^{-i\varphi_u} & 0 \\ -c_\beta M_Z s_{\theta_W} & c_\beta M_W & 0 & -\lambda \frac{v_s}{\sqrt{2}} e^{i\varphi_s} & -\frac{\sqrt{2} M_W s_\beta s_{\theta_W} \lambda e^{i\varphi_u}}{e} \\ M_Z s_\beta s_{\theta_W} e^{-i\varphi_u} & -M_W s_\beta e^{-i\varphi_u} & -\lambda \frac{v_s}{\sqrt{2}} e^{i\varphi_s} & 0 & -\frac{\sqrt{2} M_W c_\beta s_{\theta_W} \lambda}{e} \\ 0 & 0 & -\frac{\sqrt{2} M_W s_\beta s_{\theta_W} \lambda e^{i\varphi_u}}{e} & -\frac{\sqrt{2} M_W c_\beta s_{\theta_W} \lambda}{e} & \sqrt{2} \kappa v_s e^{i\varphi_s} \end{pmatrix} \quad (6)$$

where M_W and M_Z are the W and Z boson masses, respectively. The angle β is defined via the ratio of the vacuum expectation values of the two Higgs doublets, $\tan \beta = v_u/v_d$, θ_W denotes the electroweak mixing angle and e is the electric charge. From here on the short hand notation $c_x = \cos x$, $s_x = \sin x$ and $t_x = \tan x$ is used.

The neutralino mass matrix M_N is complex⁶ but symmetric and can be diagonalized with the help of the 5×5 matrix \mathcal{N} , yielding $\text{diag}(m_{\tilde{\chi}_1^0}, m_{\tilde{\chi}_2^0}, m_{\tilde{\chi}_3^0}, m_{\tilde{\chi}_4^0}, m_{\tilde{\chi}_5^0}) = \mathcal{N}^* M_N \mathcal{N}^\dagger$, where the absolute mass values are ordered as $|m_{\tilde{\chi}_1^0}| \leq \dots \leq |m_{\tilde{\chi}_5^0}|$. The neutralino mass eigenstates $\tilde{\chi}_i^0$, expressed as a Majorana spinor, can then be obtained by

$$\tilde{\chi}_i^0 = (\chi_i^0, \overline{\chi_i^0})^T \quad \text{with} \quad \chi_i^0 = \mathcal{N}_{ij} \psi_j^0, \quad i, j = 1, \dots, 5. \quad (7)$$

The fermionic superpartners of the charged Higgs and gauge bosons are given in terms of the Weyl spinors \tilde{H}_d^\pm , \tilde{H}_u^\pm , \tilde{W}_1 and \tilde{W}_2 where the latter two can be reexpressed as $\tilde{W}^\pm = (\tilde{W}_1 \mp i\tilde{W}_2)/\sqrt{2}$. Arranging these Weyl spinors as

$$\psi_R^- = \begin{pmatrix} \tilde{W}^- \\ \tilde{H}_d^- \end{pmatrix}, \quad \psi_L^+ = \begin{pmatrix} \tilde{W}^+ \\ \tilde{H}_u^+ \end{pmatrix} \quad (8)$$

leads to mass terms of the form, $(\psi_R^-)^T M_C \psi_L^+ + h.c.$, with the chargino mass matrix

$$M_C = \begin{pmatrix} M_2 & \sqrt{2} s_\beta M_W e^{-i\varphi_u} \\ \sqrt{2} c_\beta M_W & \lambda \frac{v_s}{\sqrt{2}} e^{i\varphi_s} \end{pmatrix}. \quad (9)$$

The chargino mass matrix can be diagonalized with the help of two unitary 2×2 matrices, U and V , yielding $\text{diag}(m_{\tilde{\chi}_1^\pm}, m_{\tilde{\chi}_2^\pm}) = U^* M_C V^\dagger$ with $m_{\tilde{\chi}_1^\pm} \leq m_{\tilde{\chi}_2^\pm}$. The left-handed and the right-handed part of the mass eigenstates are

$$\tilde{\chi}_L^\pm = V \psi_L^\pm, \quad \tilde{\chi}_R^\pm = U \psi_R^\pm, \quad (10)$$

respectively, with the mass eigenstates $\tilde{\chi}_i^\pm = (\tilde{\chi}_{L_i}^\pm, \overline{\tilde{\chi}_{R_i}^\pm})^T$, $i = 1, 2$, written as a Dirac spinor.

⁶Note, that in general the parameters λ , κ , M_1 and M_2 are complex.

3 The Higgs Boson Sector in the Complex NMSSM

3.1 The Higgs Boson Sector at Tree-Level

To ensure the minimum of the Higgs potential V_{Higgs} at non-vanishing vacuum expectation values v_u, v_d, v_s the terms linear in the Higgs boson fields have to vanish according to

$$t_\phi \equiv \frac{\partial V_{\text{Higgs}}}{\partial \phi} \Big|_{\text{Min.}} \stackrel{!}{=} 0 \quad \text{for} \quad \phi = h_d, h_u, h_s, a_d, a_u, a_s. \quad (11)$$

At tree-level, these tadpole parameters t_ϕ are given by⁷

$$t_{h_d} = \left[m_{H_d}^2 + \frac{M_Z^2 c_{2\beta}}{2} - v_s t_\beta |\lambda| \left(\frac{|A_\lambda|}{\sqrt{2}} c_{\varphi_x} + |\kappa| \frac{v_s}{2} c_{\varphi_y} \right) + |\lambda|^2 \left(\frac{2s_\beta^2 M_W^2 s_{\theta_W}^2}{e^2} + \frac{v_s^2}{2} \right) \right] \frac{2c_\beta M_W s_{\theta_W}}{e}, \quad (12)$$

$$t_{h_u} = \left[m_{H_u}^2 - \frac{M_Z^2 c_{2\beta}}{2} - \frac{|\lambda| v_s}{t_\beta} \left(\frac{|A_\lambda|}{\sqrt{2}} c_{\varphi_x} + |\kappa| \frac{v_s}{2} c_{\varphi_y} \right) + |\lambda|^2 \left(\frac{2c_\beta^2 M_W^2 s_{\theta_W}^2}{e^2} + \frac{v_s^2}{2} \right) \right] \frac{2s_\beta M_W s_{\theta_W}}{e}, \quad (13)$$

$$t_{h_s} = m_S^2 v_s - \left[s_{2\beta} |\lambda| \left(\frac{|A_\lambda|}{\sqrt{2}} c_{\varphi_x} + |\kappa| v_s c_{\varphi_y} \right) - |\lambda|^2 v_s \right] \frac{2M_W^2 s_{\theta_W}^2}{e^2} + |\kappa|^2 v_s^3 + \frac{1}{\sqrt{2}} |A_\kappa| |\kappa| v_s^2 c_{\varphi_z}, \quad (14)$$

$$t_{a_d} = \frac{M_W s_{\theta_W} s_\beta}{e} |\lambda| v_s (\sqrt{2} |A_\lambda| s_{\varphi_x} - |\kappa| v_s s_{\varphi_y}), \quad (15)$$

$$t_{a_u} = \frac{1}{t_\beta} t_{a_d}, \quad (16)$$

$$t_{a_s} = \frac{2M_W^2 s_{\theta_W}^2 s_{2\beta}}{e^2} |\lambda| \left(\frac{1}{\sqrt{2}} |A_\lambda| s_{\varphi_x} + |\kappa| v_s s_{\varphi_y} \right) - \frac{1}{\sqrt{2}} |A_\kappa| |\kappa| v_s^2 s_{\varphi_z}, \quad (17)$$

where we have introduced a short hand notation for the following phase combinations

$$\varphi_x = \varphi_{A_\lambda} + \varphi_\lambda + \varphi_s + \varphi_u, \quad (18)$$

$$\varphi_y = \varphi_\kappa - \varphi_\lambda + 2\varphi_s - \varphi_u, \quad (19)$$

$$\varphi_z = \varphi_{A_\kappa} + \varphi_\kappa + 3\varphi_s. \quad (20)$$

In the expressions for the tadpole parameters some of the original parameters have already been replaced in favour of the parameters on which we will impose our renormalization conditions, as described in detail in Sects. 3.2 and 3.3. Thus the vacuum expectation values v_u, v_d and the $U(1)$ and $SU(2)$ gauge couplings g' and g have been replaced by $\tan \beta = v_u/v_d$, the gauge boson masses M_W and M_Z and the electric charge e (according to Eqs. (124) and (125) in Appendix A). This replacement has also been applied in the expressions of the mass matrices given below.

It should be noted that the Eqs. (15) and (17) can have zero, one or two solutions for $\varphi_x, \varphi_z \in [-\pi, \pi)$ depending on the values of the parameters. If no solution is found there is no minimum of the Higgs potential at the corresponding set of values v_d, v_u, v_s and thus this parameter point is discarded. The single solutions yield one of the two values $\varphi_x, \varphi_z = \pm\pi/2$. Assuming there exist two solutions of Eq. (15) then if φ_x^S with $\varphi_x^S > 0$ solves this equation then also $\pi - \varphi_x^S$ is a solution and similarly if φ_x^S with $\varphi_x^S < 0$ is a solution then $-(\pi - \varphi_x^S)$ is the second solution, analogously for φ_z^S .

⁷The complex parameters are expressed in terms of their absolute value and a complex phase, *i.e.* for example $\lambda \equiv |\lambda| e^{i\varphi_\lambda}$.

The terms of the Higgs potential which are bilinear in the neutral Higgs boson fields contribute to the corresponding 6×6 Higgs boson mass matrix $M_{\phi\phi}$ in the basis of $\phi = (h_d, h_u, h_s, a_d, a_u, a_s)^T$ which can be expressed in terms of three 3×3 matrices M_{hh} , M_{aa} and M_{ha}

$$M_{\phi\phi} = \begin{pmatrix} M_{hh} & M_{ha} \\ M_{ha}^T & M_{aa} \end{pmatrix} \quad (21)$$

where M_{hh} and M_{aa} are symmetric matrices.

The entries of M_{hh} describing the mixing of the CP-even components of the Higgs doublet and singlet fields read

$$M_{h_d h_d} = M_Z^2 c_\beta^2 + \frac{1}{2} |\lambda| v_s t_\beta (\sqrt{2} |A_\lambda| c_{\varphi_x} + |\kappa| v_s c_{\varphi_y}) , \quad (22)$$

$$M_{h_d h_u} = -\frac{1}{2} M_Z^2 s_{2\beta} - \frac{1}{2} |\lambda| v_s (\sqrt{2} |A_\lambda| c_{\varphi_x} + |\kappa| v_s c_{\varphi_y}) + 2 |\lambda|^2 \frac{M_W^2 s_{\theta_W}^2}{e^2} s_{2\beta} , \quad (23)$$

$$M_{h_u h_u} = M_Z^2 s_\beta^2 + \frac{1}{2} |\lambda| \frac{v_s}{t_\beta} (\sqrt{2} |A_\lambda| c_{\varphi_x} + |\kappa| v_s c_{\varphi_y}) , \quad (24)$$

$$M_{h_d h_s} = 2 |\lambda|^2 \frac{M_W s_{\theta_W}}{e} c_\beta v_s - |\lambda| \frac{M_W s_{\theta_W}}{e} s_\beta (\sqrt{2} |A_\lambda| c_{\varphi_x} + 2 |\kappa| v_s c_{\varphi_y}) , \quad (25)$$

$$M_{h_u h_s} = 2 |\lambda|^2 \frac{M_W s_{\theta_W}}{e} s_\beta v_s - |\lambda| \frac{M_W s_{\theta_W}}{e} c_\beta (\sqrt{2} |A_\lambda| c_{\varphi_x} + 2 |\kappa| v_s c_{\varphi_y}) , \quad (26)$$

$$M_{h_s h_s} = 2 |\kappa|^2 v_s^2 + \frac{v_s}{\sqrt{2}} |\kappa| |A_\kappa| c_{\varphi_z} + \sqrt{2} |A_\lambda| |\lambda| \frac{M_W^2 s_{\theta_W}^2}{e^2 v_s} s_{2\beta} c_{\varphi_x} . \quad (27)$$

Note, that here the tadpole conditions Eqs. (12)–(14) together with Eq. (11) have already been applied to eliminate $m_{H_d}^2$, $m_{H_u}^2$ and m_S^2 . Exploiting additionally Eqs. (15) and (17) we can eliminate c_{φ_x} and c_{φ_z} through

$$c_{\varphi_x} = \pm \sqrt{1 - \frac{|\kappa|^2 v_s^2}{2 |A_\lambda|^2} s_{\varphi_y}^2} , \quad (28)$$

$$c_{\varphi_z} = \pm \sqrt{1 - 18 \frac{M_W^4 s_{\theta_W}^4 s_{2\beta}^2 |\lambda|^2}{e^4 |A_\kappa|^2 v_s^2} s_{\varphi_y}^2} . \quad (29)$$

The two signs correspond to the two possible solutions of Eqs. (15) and (17) (as explained before). Choosing either solution will define the sign of the cosine. In our numerical evaluation we will treat the sign as a further input.

The mixing of the CP-odd components of the Higgs doublet and singlet fields is characterized by the matrix M_{aa} which has the following entries,

$$M_{a_d a_d} = \frac{1}{2} |\lambda| (\sqrt{2} |A_\lambda| c_{\varphi_x} + |\kappa| v_s c_{\varphi_y}) v_s t_\beta , \quad (30)$$

$$M_{a_d a_u} = \frac{1}{2} |\lambda| (\sqrt{2} |A_\lambda| c_{\varphi_x} + |\kappa| v_s c_{\varphi_y}) v_s , \quad (31)$$

$$M_{a_u a_u} = \frac{1}{2} |\lambda| (\sqrt{2} |A_\lambda| c_{\varphi_x} + |\kappa| v_s c_{\varphi_y}) \frac{v_s}{t_\beta} , \quad (32)$$

$$M_{a_d a_s} = |\lambda| \frac{M_W s_{\theta_W}}{e} s_\beta (\sqrt{2} |A_\lambda| c_{\varphi_x} - 2 |\kappa| v_s c_{\varphi_y}) , \quad (33)$$

$$M_{a_u a_s} = |\lambda| \frac{M_W s_{\theta_W}}{e} c_\beta (\sqrt{2} |A_\lambda| c_{\varphi_x} - 2 |\kappa| v_s c_{\varphi_y}) , \quad (34)$$

$$M_{a_s a_s} = |\lambda| (\sqrt{2} |A_\lambda| c_{\varphi_x} + 4 |\kappa| v_s c_{\varphi_y}) \frac{M_W^2 s_{\theta_W}^2}{e^2 v_s} s_{2\beta} - 3 |A_\lambda| |\kappa| \frac{v_s}{\sqrt{2}} c_{\varphi_z} , \quad (35)$$

where again Eq. (11) together with the Eqs. (12)–(14) have been applied and Eqs. (11), (15) and (17) can be used to replace c_{φ_x} and c_{φ_z} . The matrix M_{ha} governs the mixing between the CP-even and the CP-odd components of the Higgs doublet and singlet fields,

$$M_{ha} = \begin{pmatrix} 0 & 0 & 3v_s s_\beta \\ 0 & 0 & 3v_s c_\beta \\ -v_s s_\beta & -v_s c_\beta & -4s_{2\beta} \frac{M_W s_{\theta_W}}{e} \end{pmatrix} \frac{M_W s_{\theta_W}}{e} |\kappa| |\lambda| s_{\varphi_y} . \quad (36)$$

In case of $\varphi_y = n_y \pi$, $n_y \in \mathbb{Z}$, the entries of M_{ha} vanish and hence, in that case, there is no CP violation at tree-level in the NMSSM Higgs sector; after transformation to the mass eigenstates we are left with three purely CP-even and two purely CP-odd Higgs bosons.

The transformation into mass eigenstates can be performed in two steps. In our approach, first, the Goldstone boson field is extracted by applying the 6×6 rotation matrix⁸ \mathcal{R}^G ,

$$\Phi_i = \mathcal{R}_{ij}^G \phi_j , \quad (37)$$

where $\Phi = (h_d, h_u, h_s, A, a_s, G)^T$. The resulting mass matrix,

$$M_{\Phi\Phi} = \mathcal{R}^G M_{\phi\phi} \mathcal{R}^{G^T} , \quad (38)$$

can finally be diagonalized with the help of the matrix \mathcal{R} leading to

$$\mathcal{R} M_{\Phi\Phi} \mathcal{R}^T = \text{diag} \left((M_{H_1}^{(0)})^2, \dots, (M_{H_5}^{(0)})^2, 0 \right) =: \mathcal{D}_H \quad (39)$$

with the mass values being ordered as $M_{H_1}^{(0)} \leq \dots \leq M_{H_5}^{(0)}$ and the superscript (0) denoting the tree-level values of the masses. The corresponding mass eigenstates are obtained as

$$H_i = \mathcal{R}_{ij} \Phi_j . \quad (40)$$

The mass matrix $M_{h^+ h^-}$ of the charged entries of the Higgs doublet fields,

$$(h_d^+, h_u^+) M_{h^+ h^-} (h_d^-, h_u^-)^T , \quad (41)$$

is explicitly given as

$$M_{h^+ h^-} = \frac{1}{2} \begin{pmatrix} t_\beta & 1 \\ 1 & \frac{1}{t_\beta} \end{pmatrix} \left[M_W^2 s_{2\beta} + |\lambda| v_s (\sqrt{2} |A_\lambda| c_{\varphi_x} + |\kappa| v_s c_{\varphi_y}) - 2 |\lambda|^2 \frac{M_W^2 s_{\theta_W}^2}{e^2} s_{2\beta} \right] , \quad (42)$$

where again the Eqs. (11)–(14) have already been applied. Diagonalizing this mass matrix with the help of a rotation matrix with the angle β_c , where $\beta_c = \beta$ at tree-level, yields the mass of the physical charged Higgs boson,

$$M_{H^\pm}^2 = M_W^2 + \frac{|\lambda| v_s}{s_{2\beta}} (\sqrt{2} |A_\lambda| c_{\varphi_x} + |\kappa| v_s c_{\varphi_y}) - 2 |\lambda|^2 \frac{M_W^2 s_{\theta_W}^2}{e^2} , \quad (43)$$

and a mass of zero for the charged Goldstone boson.

⁸The explicit form of \mathcal{R}^G can be found in Appendix B.

3.2 Set of Input Parameters for the Higgs Boson Sector

To summarize, the original parameters entering the Higgs potential and thereby also the Higgs mass matrix are

$$m_{H_d}^2, m_{H_u}^2, m_S^2, \varphi_{A_\kappa}, \varphi_{A_\lambda}, |A_\lambda|, g, g', v_u, v_d, v_s, \varphi_s, \varphi_u, |\lambda|, \varphi_\lambda, |\kappa|, \varphi_\kappa, |A_\kappa|. \quad (44)$$

Instead of using this set of original parameters it is convenient to convert it to a set of parameters which offer an intuitive interpretation. This is especially true for the parameters which can be replaced by gauge boson masses squared as they are measurable quantities. We have chosen the set,

$$\underbrace{t_{h_d}, t_{h_u}, t_{h_s}, t_{a_d}, t_{a_s}, M_{H^\pm}^2, M_W^2, M_Z^2, e}_{\text{on-shell}} \underbrace{\tan \beta, v_s, \varphi_s, \varphi_u, |\lambda|, \varphi_\lambda, |\kappa|, \varphi_\kappa, |A_\kappa|}_{\overline{\text{DR}}} \quad (45)$$

where the first part of the parameters are directly related to ‘‘physical’’ quantities⁹ and will be defined via on-shell conditions while the remaining parameters are understood as $\overline{\text{DR}}$ parameters (see Sect. 3.3.2). The transformation rules for going from set Eq. (44) to set Eq. (45) are given in Appendix A.

3.3 The Higgs Boson Sector at One-Loop Level

At one-loop level, the Higgs boson sector and the corresponding relations between parameters of the theory and physical quantities are changed by radiative corrections. In particular, the Higgs boson mass matrix receives contributions from the renormalized self-energies¹⁰ $\hat{\Sigma}_{ij}(p^2)$ at an external momentum squared p^2 ,

$$\hat{\Sigma}_{ij}(p^2) = \Sigma_{ij}(p^2) + \frac{1}{2}p^2 \left[\delta\mathcal{Z}^\dagger + \delta\mathcal{Z} \right]_{ij} - \frac{1}{2} \left[\delta\mathcal{Z}^\dagger \mathcal{D}_H + \mathcal{D}_H^\dagger \delta\mathcal{Z} \right]_{ij} - [\mathcal{R}\delta\mathcal{M}_{\Phi\Phi}\mathcal{R}^\dagger]_{ij}, \quad (46)$$

with $i, j = 1, \dots, 6$ and $H_6 = G$ the Goldstone boson. The unrenormalized self-energies Σ_{ij} are obtained by taking into account all possible contributions to the Higgs boson self-energy, including the ones from fermion, gauge boson, Goldstone boson, Higgs boson, chargino, neutralino, sfermion and ghost loops.

The wave function renormalization matrix $\delta\mathcal{Z}$ in the basis of the Higgs boson mass eigenstates is derived via rotation from the corresponding matrix $\delta\mathcal{Z}_\Phi$ in the basis of the Higgs boson states Φ ,

$$\delta\mathcal{Z} = \mathcal{R}\delta\mathcal{Z}_\Phi\mathcal{R}^\dagger. \quad (47)$$

The Higgs boson fields Φ are renormalized by replacing the fields by renormalized ones and a renormalization factor. This can be expressed as, valid up to one-loop order, with the field renormalization constant $\delta\mathcal{Z}_\Phi$ as

$$\Phi \rightarrow \left(\mathbb{1} + \frac{1}{2}\delta\mathcal{Z}_\Phi \right) \Phi, \quad (48)$$

⁹Whether the tadpole parameters can be called physical quantities is debatable but certainly their introduction is motivated by physical interpretation. Therefore, in a slight abuse of the language, we are also calling the renormalization conditions for the tadpole parameters on-shell.

¹⁰In general, we call $\hat{\Sigma}$ and Σ renormalized and unrenormalized self-energy, respectively.

where $\delta\mathcal{Z}_\Phi = \mathcal{R}^G \delta\mathcal{Z}_\phi \mathcal{R}^{G\dagger}$. The field renormalization constant $\delta\mathcal{Z}^\phi$ of the interaction eigenstates ϕ is a diagonal matrix

$$\delta\mathcal{Z}_\phi = \text{diag}(\delta Z_{H_u}, \delta Z_{H_d}, \delta Z_S, \delta Z_{H_d}, \delta Z_{H_u}, \delta Z_S) . \quad (49)$$

The explicit definitions and expressions for δZ_{H_u} , δZ_{H_d} and δZ_S are given in Sect. 3.3.1.

The matrix $\delta\mathcal{M}_{\Phi\Phi}$ denotes the counterterm matrix in the basis of the Higgs boson states Φ which has been introduced within the renormalization procedure by replacing the parameters in the mass matrix as given in Appendix A in Eqs. (118)–(125) by their renormalized ones and corresponding counterterms and expanding about the renormalized parameters. The part linear in the counterterms forms the mass matrix counterterm. The specific definitions of the parameters and the determination of the counterterms are discussed in Sect. 3.3.2.

3.3.1 Higgs boson field renormalization

The field renormalization constants introduced in Eq. (49) are defined in the $\overline{\text{DR}}$ scheme. The precise expressions for δZ_{H_d} , δZ_{H_u} and δZ_S are determined via the following system of equations

$$\begin{aligned} \delta Z_{H_d} (|\mathcal{R}_{i1}|^2 + |\mathcal{R}_{i4} \sin \beta + \mathcal{R}_{i6} \cos \beta|^2) + \delta Z_{H_u} (|\mathcal{R}_{i2}|^2 + |\mathcal{R}_{i4} \cos \beta - \mathcal{R}_{i6} \sin \beta|^2) \\ + \delta Z_S (|\mathcal{R}_{i3}|^2 + |\mathcal{R}_{i5}|^2) = -\Sigma'_{ii}|_{\text{div}} \quad \text{with } i = 1, 2, 3 , \end{aligned} \quad (50)$$

where

$$\Sigma'_{ii} = \left. \frac{\partial \Sigma_{ii}(p^2)}{\partial p^2} \right|_{p^2=(M_{H_i}^{(0)})^2} . \quad (51)$$

The subscript 'div' denotes that only the divergent parts proportional to Δ are taken into account with $\Delta = 2/(4-D) - \gamma_E + \ln 4\pi$ and γ_E being the Euler constant and D the number of dimensions. The pole of Δ for $D = 4$ characterizes the divergences. Solving this system of equations Eq. (50) yields

$$\delta Z_{H_d} = \frac{1}{r} [(r_{23}r_{32} - r_{22}r_{33})\Sigma'_{11} + (r_{12}r_{33} - r_{13}r_{32})\Sigma'_{22} + (r_{13}r_{22} - r_{12}r_{23})\Sigma'_{33}]_{\text{div}} , \quad (52)$$

$$\delta Z_{H_u} = \frac{1}{r} [(r_{21}r_{33} - r_{23}r_{31})\Sigma'_{11} + (r_{13}r_{31} - r_{11}r_{33})\Sigma'_{22} + (r_{11}r_{23} - r_{13}r_{21})\Sigma'_{33}]_{\text{div}} , \quad (53)$$

$$\delta Z_S = \frac{1}{r} [(r_{22}r_{31} - r_{21}r_{32})\Sigma'_{11} + (r_{11}r_{32} - r_{12}r_{31})\Sigma'_{22} + (r_{12}r_{21} - r_{11}r_{22})\Sigma'_{33}]_{\text{div}} , \quad (54)$$

with

$$r_{i1} = (|\mathcal{R}_{i1}|^2 + |\mathcal{R}_{i4} \sin \beta + \mathcal{R}_{i6} \cos \beta|^2) , \quad (55)$$

$$r_{i2} = (|\mathcal{R}_{i2}|^2 + |\mathcal{R}_{i4} \cos \beta - \mathcal{R}_{i6} \sin \beta|^2) , \quad (56)$$

$$r_{i3} = (|\mathcal{R}_{i3}|^2 + |\mathcal{R}_{i5}|^2) , \quad (57)$$

$$r = r_{11}r_{22}r_{33} + r_{12}r_{23}r_{31} + r_{13}r_{32}r_{21} - r_{11}r_{23}r_{32} - r_{13}r_{22}r_{31} - r_{12}r_{21}r_{33} . \quad (58)$$

It should be noted that $\mathcal{R}_{i6} = 0$ for $i \neq 6$ and hence, in Eqs. (55) and (56) terms proportional to \mathcal{R}_{i6} vanish for the values $i = 1, 2, 3$ needed in Eqs. (52)–(54).

3.3.2 Parameter renormalization

The parameter renormalization is performed by replacing the parameters by the renormalized ones and the corresponding counterterms,

$$t_\phi \rightarrow t_\phi + \delta t_\phi \quad \text{with } \phi = \{h_d, h_u, h_s, a_d, a_s\}, \quad (59)$$

$$M_{H^\pm}^2 \rightarrow M_{H^\pm}^2 + \delta M_{H^\pm}^2, \quad M_W^2 \rightarrow M_W^2 + \delta M_W^2, \quad M_Z^2 \rightarrow M_Z^2 + \delta M_Z^2, \quad (60)$$

$$e \rightarrow (1 + \delta Z_e)e, \quad (61)$$

$$\tan \beta \rightarrow \tan \beta + \delta \tan \beta, \quad v_s \rightarrow v_s + \delta v_s, \quad (62)$$

$$\varphi_s \rightarrow \varphi_s + \delta \varphi_s, \quad \varphi_u \rightarrow \varphi_u + \delta \varphi_u, \quad (63)$$

$$\lambda \rightarrow \lambda + \delta \lambda = \lambda + e^{i\varphi_\lambda} \delta |\lambda| + i\lambda \delta \varphi_\lambda, \quad \kappa \rightarrow \kappa + \delta \kappa = \kappa + e^{i\varphi_\kappa} \delta |\kappa| + i\kappa \delta \varphi_\kappa, \quad (64)$$

$$|A_\kappa| \rightarrow |A_\kappa| + \delta |A_\kappa|. \quad (65)$$

In the case of complex parameters the complex counterterms can be understood in terms of two real counterterms, one for the absolute value and one for the phase, as in Eq. (64) for $\delta \lambda$ and $\delta \kappa$.

As we make use of the chargino and the neutralino sector for the determination of the counterterms δv_s , $\delta \varphi_s$, $\delta \lambda$, $\delta \kappa$ and $\delta \varphi_u$ we also need to renormalize the gaugino mass parameters M_1 and M_2 ,

$$M_1 \rightarrow M_1 + \delta M_1 = M_1 + e^{i\varphi_{M_1}} \delta |M_1| + iM_1 \delta \varphi_{M_1}, \quad (66)$$

$$M_2 \rightarrow M_2 + \delta M_2 = M_2 + e^{i\varphi_{M_2}} \delta |M_2| + iM_2 \delta \varphi_{M_2}. \quad (67)$$

To keep the relations as general as possible we do not make use of the R -symmetry relations here and keep both gaugino mass parameters complex.

In the following, we list all the renormalization conditions and counterterms. The renormalization scheme applied here is a generalization of the ‘‘mixed scheme’’ of Ref. [26] for complex parameters – we will be brief on the conditions that can be directly taken from Ref. [26].

(i-v) Tadpole parameters:

The renormalization conditions for the tadpole parameters are chosen such that the linear terms of the Higgs boson fields in the Higgs potential also vanish at one-loop level,

$$\delta t_\phi = T_\phi \quad \text{with } \phi = h_d, h_u, h_s, a_d, a_s, \quad (68)$$

where T_ϕ denotes the contribution of the irreducible one-loop tadpole diagrams.

(vi - viii) Masses of the gauge bosons and the charged Higgs boson:

The masses of the gauge bosons and of the charged Higgs boson are determined via on-shell conditions requiring that the mass parameters squared correspond to the pole masses squared leading to

$$\delta M_W^2 = \widetilde{\text{Re}} \Sigma_{WW}^T(M_W^2), \quad \delta M_Z^2 = \widetilde{\text{Re}} \Sigma_{ZZ}^T(M_Z^2), \quad \delta M_{H^\pm}^2 = \widetilde{\text{Re}} \Sigma_{H^\mp H^\pm}(M_{H^\pm}^2), \quad (69)$$

where Σ_{WW}^T and Σ_{ZZ}^T are the transverse parts of the unrenormalized W boson and Z boson self-energy, respectively, while $\Sigma_{H^\mp H^\pm}$ denotes the unrenormalized self-energy of the charged Higgs boson. $\widetilde{\text{Re}}$ takes only the real part of the scalar loop functions but keeps the complex structure of the parameters.

(ix) Electric charge:

The electric charge is fixed via the $e\bar{e}\gamma$ vertex in such a way that this vertex does not receive any corrections at the one-loop level in the Thomson limit, *i.e.* for zero momentum transfer. This yields (*cf.* Ref. [30] up to a different sign convention in the second term)

$$\delta Z_e = \frac{1}{2} \Sigma_{\gamma\gamma}^{T'}(0) + \frac{s_{\theta_W}}{c_{\theta_W} M_Z^2} \Sigma_{\gamma Z}^T(0) , \quad (70)$$

with $\Sigma_{\gamma\gamma}^T$ and $\Sigma_{\gamma Z}^T$ being the transverse part of the unrenormalized photon self-energy and the unrenormalized mixing of photon and Z boson, respectively.

(x) Ratio of the vacuum expectation values $\tan\beta$:

The ratio of the vacuum expectation values $\tan\beta$ is defined as a $\overline{\text{DR}}$ parameter and the counterterm is given by [31, 32]

$$\delta \tan\beta = \frac{\tan\beta}{2} [\delta Z_{H_u} - \delta Z_{H_d}]|_{\text{div}} . \quad (71)$$

(xi,xii) Vacuum expectation value v_s and phase φ_s :

The singlet vacuum expectation value v_s and the phase φ_s are determined as $\overline{\text{DR}}$ parameters. For the derivation of the corresponding counterterms, we start out from the on-shell conditions for the chargino masses,

$$\widetilde{\text{Re}} \hat{\Sigma}_{\chi_{ii}^+}(p) \tilde{\chi}_i^+(p)|_{p^2=m_{\chi_{ii}^\pm}^2} = 0, \quad i = 1, 2, \quad (72)$$

where $\hat{\Sigma}_{\chi_{ii}^+}$ are the renormalized chargino self-energies. Applying the decomposition of the fermionic self-energy

$$\hat{\Sigma}_{ij}(p^2) = \not{p} \hat{\Sigma}_{ij}^L(p^2) \mathcal{P}_L + \not{p} \hat{\Sigma}_{ij}^R(p^2) \mathcal{P}_R + \hat{\Sigma}_{ij}^{Ls}(p^2) \mathcal{P}_L + \hat{\Sigma}_{ij}^{Rs}(p^2) \mathcal{P}_R \quad (73)$$

with $\mathcal{P}_{L,R} = (1 \mp \gamma_5)/2$ being the left- and right-handed projectors, leads to the finite relations

$$[m_{\tilde{\chi}_i^\pm} (\widetilde{\text{Re}} \hat{\Sigma}_{\chi^\pm}^L(p^2) + \widetilde{\text{Re}} \hat{\Sigma}_{\chi^\pm}^R(p^2)) + \widetilde{\text{Re}} \hat{\Sigma}_{\chi^\pm}^{Ls}(p^2) + \widetilde{\text{Re}} \hat{\Sigma}_{\chi^\pm}^{Rs}(p^2)]_{ii} = 0 , \quad (74)$$

$$[m_{\tilde{\chi}_i^\pm} (\widetilde{\text{Re}} \hat{\Sigma}_{\chi^\pm}^L(p^2) - \widetilde{\text{Re}} \hat{\Sigma}_{\chi^\pm}^R(p^2)) - \widetilde{\text{Re}} \hat{\Sigma}_{\chi^\pm}^{Ls}(p^2) + \widetilde{\text{Re}} \hat{\Sigma}_{\chi^\pm}^{Rs}(p^2)]_{ii} = 0 , \quad (75)$$

which can be exploited for the determination of the counterterms. Using the expressions given in Eqs. (143)–(146) in Appendix C for the renormalized self-energies yields

$$\begin{aligned} \text{Re}(U^* \delta M_C V^\dagger)|_{\text{div}} &= \frac{1}{2} [m_{\tilde{\chi}_i^\pm} (\Sigma_{\chi^+}^L(p^2) + \Sigma_{\chi^+}^R(p^2)) + \Sigma_{\chi^+}^{Ls}(p^2) + \Sigma_{\chi^+}^{Rs}(p^2)]_{ii}|_{\text{div}} \\ &=: \text{Re } \delta m_{\chi_{ii}^+} , \end{aligned} \quad (76)$$

$$\begin{aligned} \text{Im}(U^* \delta M_C V^\dagger)|_{\text{div}} &= \frac{i}{2} [\Sigma_{\chi^+}^{Rs}(p^2) - \Sigma_{\chi^+}^{Ls}(p^2) + i m_{\tilde{\chi}_i^\pm} (U^* \text{Im} \delta Z_R^C U^T + V \text{Im} \delta Z_L^C V^\dagger)]_{ii}|_{\text{div}} \\ &=: \text{Im } \delta m_{\chi_{ii}^+} . \end{aligned} \quad (77)$$

The imaginary parts of the field renormalization constants have been set to zero, hence $\text{Im} \delta Z_R^C = \text{Im} \delta Z_L^C = 0$. With

$$\delta M_C = \begin{pmatrix} \delta M_2 & \sqrt{2} e^{-i\varphi_u} [\delta(M_W s_\beta) - i s_\beta M_W \delta\varphi_u] \\ \sqrt{2} \delta(c_\beta M_W) & \frac{e^{i\varphi_s}}{\sqrt{2}} [\lambda \delta v_s + i \lambda v_s \delta\varphi_s + v_s \delta\lambda] \end{pmatrix} , \quad (78)$$

solving Eqs. (76) and (77) for $\delta v_s + iv_s \delta \varphi_s$ and δM_2 ¹¹, we obtain

$$\delta M_2 = \frac{1}{|U_{11}|^2 - |V_{12}|^2} [V_{11}U_{11}\delta m_{\chi_{11}^+} - V_{21}U_{21}\delta m_{\chi_{22}^+} - U_{11}U_{12}^*\delta M_{C_{21}}|_{\text{div}} - V_{11}V_{12}^*\delta M_{C_{12}}|_{\text{div}}] , \quad (79)$$

$$\delta v_s + iv_s \delta \varphi_s = \frac{\sqrt{2}\lambda^* e^{-i\varphi_s}}{|\lambda|^2(|U_{11}|^2 - |V_{12}|^2)} [-V_{12}U_{12}\delta m_{\chi_{11}^+} + V_{22}U_{22}\delta m_{\chi_{22}^+} + U_{11}^*U_{12}\delta M_{C_{12}}|_{\text{div}} + V_{11}^*V_{12}\delta M_{C_{21}}|_{\text{div}}] - v_s \lambda^* \frac{\delta \lambda}{|\lambda|^2} . \quad (80)$$

It should be noted that $\delta \varphi_u$ contained in $\delta M_{C_{12}}$ as well as $\delta \lambda$ have not been defined yet. We need additional conditions given by Eqs. (98)–(100). Together with Eqs. (79) and (80) they form a system of linear equations that can be easily solved but leads to lengthy expressions.

(xiii – xvii) Couplings λ and κ and the phase φ_u :

The phase φ_u as well as λ and κ are also defined as $\overline{\text{DR}}$ parameters. On-shell conditions for the neutralino masses¹²

$$\widetilde{\text{Re}}\hat{\Sigma}_{\chi_{ii}^0}(p)\tilde{\chi}_i^0(p)|_{p^2=m_{\chi_i^0}^2} = 0, \quad i = 1, \dots, 4 , \quad (81)$$

are exploited to derive the following finite relations,¹³

$$[m_{\tilde{\chi}_i^0}(\widetilde{\text{Re}}\hat{\Sigma}_{\chi_0^0}^L(p^2) + \widetilde{\text{Re}}\hat{\Sigma}_{\chi_0^0}^R(p^2)) + \widetilde{\text{Re}}\hat{\Sigma}_{\chi_0^0}^{Ls}(p^2) + \widetilde{\text{Re}}\hat{\Sigma}_{\chi_0^0}^{Rs}(p^2)]_{ii} = 0 , \quad (82)$$

$$[m_{\tilde{\chi}_i^0}(\widetilde{\text{Re}}\hat{\Sigma}_{\chi_0^0}^L(p^2) - \widetilde{\text{Re}}\hat{\Sigma}_{\chi_0^0}^R(p^2)) - \widetilde{\text{Re}}\hat{\Sigma}_{\chi_0^0}^{Ls}(p^2) + \widetilde{\text{Re}}\hat{\Sigma}_{\chi_0^0}^{Rs}(p^2)]_{ii} = 0 , \quad (83)$$

with $i = 1, \dots, 4$. Applying the Eqs. (150)–(153) in Appendix C leads to

$$\text{Re}(\mathcal{N}^* \delta M_N \mathcal{N}^\dagger)_{ii}|_{\text{div}} = [m_{\tilde{\chi}_i^0} \Sigma_{\chi_0^0}^L(p^2) + \frac{1}{2}(\Sigma_{\chi_0^0}^{Ls}(p^2) + \Sigma_{\chi_0^0}^{Rs}(p^2))]_{ii}|_{\text{div}} =: \text{Re} \delta m_{\chi_{ii}^0} , \quad (84)$$

$$\begin{aligned} \text{Im}(\mathcal{N}^* \delta M_N \mathcal{N}^\dagger)_{ii}|_{\text{div}} &= \frac{i}{2} [\Sigma_{\chi_0^0}^{Rs}(p^2) - \Sigma_{\chi_0^0}^{Ls}(p^2) + 2im_{\tilde{\chi}_j^0}(\mathcal{N}^* \text{Im} \delta Z^N \mathcal{N}^\dagger)]_{ii}|_{\text{div}} \\ &=: \text{Im} \delta m_{\chi_{ii}^0} , \end{aligned} \quad (85)$$

$i = 1, \dots, 4$ where already $\Sigma_{\chi_0^0}^L|_{ii} = \Sigma_{\chi_0^0}^R|_{ii}$ has been used which is true due to the Majorana character of the neutralinos. The imaginary part of δZ^N has been set to zero, $\text{Im} \delta Z^N = 0$. The elements of the mass matrix counterterm δM_N are derived as

$$\delta M_{N_{11}} = \delta M_1 , \quad (86)$$

$$\delta M_{N_{22}} = \delta M_2 , \quad (87)$$

¹¹Even though M_2 does not enter the Higgs boson sector at tree-level, it has to be dealt with due to its entanglement in Eq. (78).

¹²In terms of an on-shell scheme, if both chargino masses were defined on-shell only three of the neutralino masses could be chosen independently. Although Eq. (81) leads to two independent equations for each i , for $i = 4$ it is only partly used to fix one still undefined phase.

¹³It should be noted that, in general, both Eqs. (82) and (83) for $i = 4$ only hold for the divergent part simultaneously as all the parameters are already fixed by other conditions.

$$\delta M_{N_{55}} = \sqrt{2}e^{i\varphi_s} [v_s \delta \kappa + \kappa \delta v_s + i\kappa v_s \delta \varphi_s] , \quad (88)$$

$$\delta M_{N_{13}} = -M_Z s_{\theta_W} c_\beta^2 s_\beta \delta \tan \beta + \frac{c_\beta}{2s_{\theta_W} M_Z} [\delta M_W^2 - \delta M_Z^2] , \quad (89)$$

$$\delta M_{N_{14}} = e^{-i\varphi_u} [\delta(s_\beta M_Z s_{\theta_W}) - i s_\beta M_Z s_{\theta_W} \delta \varphi_u] , \quad (90)$$

$$\delta M_{N_{23}} = \delta(c_\beta M_W) , \quad (91)$$

$$\delta M_{N_{24}} = -e^{-i\varphi_u} [\delta(s_\beta M_W) - i s_\beta M_W \delta \varphi_u] , \quad (92)$$

$$\delta M_{N_{34}} = -\frac{1}{\sqrt{2}} e^{i\varphi_s} [v_s \delta \lambda + \lambda \delta v_s + i\lambda v_s \delta \varphi_s] , \quad (93)$$

$$\delta M_{N_{35}} = -\sqrt{2} e^{i\varphi_u} \left[\lambda \frac{\delta(s_\beta M_W s_{\theta_W})}{e} - \frac{s_\beta M_W s_{\theta_W}}{e} (\lambda \delta Z_e - \delta \lambda - i\lambda \delta \varphi_u) \right] , \quad (94)$$

$$\delta M_{N_{45}} = -\sqrt{2} \left[\lambda \frac{\delta(c_\beta M_W s_{\theta_W})}{e} + \frac{c_\beta M_W s_{\theta_W}}{e} (\delta \lambda - \lambda \delta Z_e) \right] , \quad (95)$$

$$\delta M_{N_{33}} = \delta M_{N_{44}} = \delta M_{N_{12}} = \delta M_{N_{15}} = \delta M_{N_{25}} = 0 . \quad (96)$$

As the neutralino mass matrix is symmetric, this also holds for the counterterm mass matrix and therefore $\delta M_{N_{ij}} = \delta M_{N_{ji}}$. Rewriting Eqs. (84) and (85) explicitly and solving for δM_1 results in the following set of equations,

$$\begin{aligned} \delta M_1 = \frac{\mathcal{N}_{11}^2}{|\mathcal{N}_{11}|^4} & \left[\delta m_{\chi_{11}^0} - 2\mathcal{N}_{11}^* [\mathcal{N}_{13}^* \delta M_{N_{13}} + \mathcal{N}_{14}^* \delta M_{N_{14}}] - 2\mathcal{N}_{12}^* [\mathcal{N}_{13}^* \delta M_{N_{23}} + \mathcal{N}_{14}^* \delta M_{N_{24}}] \right. \\ & - 2\mathcal{N}_{13}^* [\mathcal{N}_{14}^* \delta M_{N_{34}} + \mathcal{N}_{15}^* \delta M_{N_{35}}] - 2\mathcal{N}_{14}^* \mathcal{N}_{15}^* \delta M_{N_{45}} \\ & \left. - (\mathcal{N}_{12}^*)^2 \delta M_2 - (\mathcal{N}_{15}^*)^2 \delta M_{N_{55}} \right] , \end{aligned} \quad (97)$$

$$\begin{aligned} & 2[a_{214} \delta M_{N_{14}} + a_{224} \delta M_{N_{24}} + 2a_{234} \delta M_{N_{34}} + a_{235} \delta M_{N_{35}} + a_{245} \delta M_{N_{45}}] \\ & + a_{222} \delta M_2 + a_{255} \delta M_{N_{55}} \\ & = (\mathcal{N}_{21}^*)^2 \delta m_{\chi_{11}^0} - (\mathcal{N}_{11}^*)^2 \delta m_{\chi_{22}^0} - 2a_{213} \delta M_{N_{13}} - 2a_{223} \delta M_{N_{23}} , \end{aligned} \quad (98)$$

$$\begin{aligned} & 2[a_{314} \delta M_{N_{14}} + a_{324} \delta M_{N_{24}} + 2a_{334} \delta M_{N_{34}} + a_{335} \delta M_{N_{35}} + a_{345} \delta M_{N_{45}}] \\ & + a_{322} \delta M_2 + a_{355} \delta M_{N_{55}} \\ & = (\mathcal{N}_{31}^*)^2 \delta m_{\chi_{11}^0} - (\mathcal{N}_{11}^*)^2 \delta m_{\chi_{33}^0} - 2a_{313} \delta M_{N_{13}} - 2a_{323} \delta M_{N_{23}} , \end{aligned} \quad (99)$$

$$\begin{aligned} & \text{Im} \left\{ 2[a_{414} \delta M_{N_{14}} + a_{424} \delta M_{N_{24}} + 2a_{434} \delta M_{N_{34}} + a_{435} \delta M_{N_{35}} + a_{445} \delta M_{N_{45}}] \right. \\ & \left. + a_{422} \delta M_2 + a_{455} \delta M_{N_{55}} \right\} \\ & = \text{Im} \left\{ (\mathcal{N}_{41}^*)^2 \delta m_{\chi_{11}^0} - (\mathcal{N}_{11}^*)^2 \delta m_{\chi_{44}^0} - 2a_{413} \delta M_{N_{13}} - 2a_{423} \delta M_{N_{23}} \right\} , \end{aligned} \quad (100)$$

where we have introduced the shorthand notation

$$a_{ijk} = (\mathcal{N}_{i1}^*)^2 \mathcal{N}_{1j}^* \mathcal{N}_{1k}^* - (\mathcal{N}_{11}^*)^2 \mathcal{N}_{ij}^* \mathcal{N}_{ik}^* . \quad (101)$$

As stated above, taking Eqs. (98)–(100) together with Eqs. (79) and (80) leads to a system of equations with 4 complex and one real equation linear in the counterterms that has to be solved for δM_2 , δv_s , $\delta \varphi_s$, $\delta \lambda$, $\delta \kappa$ and $\delta \varphi_u$.

(xviii) Absolute value of the singlet trilinear coupling $|A_\kappa|$:

The absolute value of the singlet trilinear coupling $|A_\kappa|$ is determined as a $\overline{\text{DR}}$ parameter.

The corresponding counterterm is calculated using

$$\mathcal{R}_{i5}\mathcal{R}_{j5}\hat{\Sigma}_{ij}(M_{a_s a_s}) = 0, \quad (102)$$

which is equivalent to

$$\delta M_{a_s a_s} = \mathcal{R}_{i5}\mathcal{R}_{j5}\Sigma_{ij}(M_{a_s a_s}), \quad (103)$$

with $\delta M_{a_s a_s}$ depending on $\delta|A_\kappa|$. Dropping the finite parts and solving for $\delta|A_\kappa|$ yields

$$\begin{aligned} \delta|A_\kappa| = & -\frac{\sqrt{2}}{|\kappa|v_s[3c_{\varphi_z} - 3t_{\varphi_z}\frac{f_2}{|A_\kappa|}]} \left\{ \mathcal{R}_{i5}\mathcal{R}_{j5}\Sigma_{ij}(M_{a_s, a_s}) - \delta f_1 \right. \\ & \left. + \frac{3}{\sqrt{2}}|A_\kappa|[v_s c_{\varphi_z} \delta|\kappa| + |\kappa|c_{\varphi_z} \delta v_s] + \frac{3}{\sqrt{2}}|\kappa|v_s t_{\varphi_z} \delta f_2 \right\}_{\text{div}} \end{aligned} \quad (104)$$

with

$$\begin{aligned} f_1 = & [M_{H^\pm}^2 - M_W^2 c_{\Delta\beta}^2] \frac{M_W^2 s_{\theta_W}^2 s_{2\beta}^2}{e^2 v_s^2 c_{\Delta\beta}^2} - \frac{M_W s_{\theta_W} s_{2\beta} c_\beta c_{\beta_B}^2}{e v_s^2 c_{\Delta\beta}^2} [t_{h_u} + t_\beta t_{\beta_B}^2 t_{h_d}] + \frac{t_{h_s}}{v_s} \\ & + |\lambda| M_W^2 \frac{s_{\theta_W}^2 s_{2\beta}}{e^2 v_s^2} [2|\lambda| M_W^2 \frac{s_{\theta_W}^2}{e^2} s_{2\beta} + 3|\kappa|v_s^2 c_{\varphi_y}], \end{aligned} \quad (105)$$

$$f_2 = \frac{\sqrt{2}}{v_s} \left(\frac{2M_W s_{\theta_W} c_\beta}{e|\kappa|v_s^2} t_{a_d} + \frac{3|\lambda| M_W^2 s_{\theta_W}^2 s_{2\beta}}{e^2} s_{\varphi_y} - \frac{1}{|\kappa|v_s} t_{a_s} \right). \quad (106)$$

The counterterms δf_1 and δf_2 , which are functions of counterterms of the parameters defined as input in Eq. (45), are determined by replacing the parameters by renormalized ones plus corresponding counterterms and expanding about the parameters. It has to be taken into account that in the expressions $\Delta\beta = \beta - \beta_B$ only β is treated within the renormalization procedure. The angle $\beta_B = \beta_c = \beta_n$ is the mixing angle of the charged Higgs bosons and the angle extracting the Goldstone boson defined in Appendix A.

Following the approach above, it has been found that the counterterms $\delta\varphi_s$, $\delta\varphi_\lambda$, $\delta\varphi_\kappa$, $\delta\varphi_u$, $\delta\varphi_{M_1}$ and $\delta\varphi_{M_2}$ vanish. In that respect, it is interesting to note that Eqs. (77) and (85) allow for a certain freedom of choice; some potentially divergent parts can be moved into $\text{Im}\delta Z_L^C$, $\text{Im}\delta Z_R^C$ and $\text{Im}\delta Z^N$ which do not appear in the calculation of the Higgs boson masses as the charginos and neutralinos only enter through internal lines in the Feynman diagrams.

The derivation of the counterterms for v_s , φ_s , λ , κ and φ_u presented above is not unique. In a second approach on-shell conditions for all the neutralino masses plus an additional condition from the chargino sector, Eq. (77) for $i = 1$, have been exploited to calculate the $\overline{\text{DR}}$ counterterms leading to the same result and providing a good cross-check. A further possibility is to determine the counterterms within the Higgs boson sector only. We have also done that but this does not test the calculation at the same level as using conditions from the chargino and neutralino sector.

3.4 Loop Corrected Higgs Boson Masses and Mixing Matrix Elements

The one-loop corrected scalar Higgs boson masses squared are extracted numerically as the zeroes of the determinant of the two-point vertex functions $\hat{\Gamma}$,

$$\hat{\Gamma}(p^2) = i(\mathbb{1} \cdot p^2 - \mathcal{M}^{11}) \quad \text{with} \quad (\mathcal{M}^{11})_{ij} = (M_{H_i}^{(0)})^2 \delta_{ij} - \hat{\Sigma}_{ij}(p^2) \quad i, j = 1, \dots, 5, \quad (107)$$

where $\hat{\Sigma}_{ij}(p^2)$ is given in Eq. (46). The superscript $1l$ denotes the one-loop order.

Starting from Eq. (107) the Higgs masses at one-loop level can be obtained via an iterative procedure.¹⁴ To calculate the one-loop mass of the n^{th} Higgs boson the external momentum squared p^2 in the renormalized self-energies $\hat{\Sigma}_{ij}$ is set equal to the tree-level mass squared ($p^2 = (M_{H_n}^{(0)})^2$) in the first iteration step. Then, the mass matrix part of $\hat{\Gamma}$, *i.e.* \mathcal{M}^{1l} , is diagonalized. The thus obtained n^{th} eigenvalue is the first approximation of the squared one-loop mass. In the next iteration step p^2 is set equal to this value and once again the eigenvalues of \mathcal{M}^{1l} are calculated to yield the next approximation of the one-loop mass. This iteration procedure is repeated until a precision of 10^{-9} is reached. All five Higgs boson masses are calculated this way.

Note that in Eq. (107) the mixing with the Goldstone bosons is not taken into account but we have checked numerically that the effect is negligible. Furthermore, it was shown in Ref. [33], that in the MSSM it is sufficient to include the mixing with the Goldstone boson, whereas the mixing with the longitudinal component of the Z boson does not have to be added explicitly. Taking into account the mixing of the Goldstone boson as well as the mixing of the Z boson leads to the same result as only including the Goldstone boson mixing.

Due to the radiative corrections, not only the masses of the particles receive contributions but at the same time the tree-level mass eigenstates mix to form new one-loop mass eigenstates. In order to take this into account the Higgs mixing matrix \mathcal{R} which performs the rotation from the interaction eigenstates to the mass eigenstates has to be adjusted so that

$$H_i^{1l} = \mathcal{R}_{ij}^{1l} \Phi_j . \quad (108)$$

In the numerical analysis, for the simplicity of the notation we drop the superscript $1l$ again. If not explicitly mentioned one-loop corrections are included.

The rotation of the tree-level to the one-loop mass eigenstates could be obtained by calculating finite wave function correction factors. The procedures to calculate these for a 2×2 or 3×3 mass matrix are described in Ref. [13] and need to be extended for the 5×5 case. Another option is to apply the $p^2 = 0$ approximation. After setting the momenta in \mathcal{M}^{1l} to zero, the rotation matrix that relates the tree-level to the one-loop mass eigenstates can be defined as the matrix that diagonalizes \mathcal{M}^{1l} . The latter procedure has the advantage that the mixing matrix is unitary. The drawback is that it does not retain the full momentum dependence. For our numerical analysis we used the $p^2 = 0$ approximation for the determination of the mixing matrix. But we checked numerically that the differences between both methods are negligible.

4 Numerical Analysis

The calculation of the one-loop corrected Higgs boson masses has been performed in two different calculations. While in one calculation the Feynman rules have been derived from the NMSSM Lagrangian and implemented in a `FeynArts` model file [34], they have been obtained with the Mathematica package `SARAH` [35] in the second calculation and cross-checked against the first calculation. The self-energies and tadpoles have been evaluated with the help of `FormCalc` [36] in the

¹⁴This procedure is not strictly of one-loop order. It was shown, however, in Ref. [32] for the MSSM that this procedure gives much exacter values for the Higgs mass including implicitly higher order corrections than a strict treatment at one-loop level.

't Hooft-Feynman gauge. The divergent integrals, regularized in the constrained differential renormalization scheme [37], have been computed numerically with `LoopTools` [36]. For the evaluation of the counterterms, numerical diagonalization of the one-loop corrected Higgs boson mass matrix and the determination of the mass eigenvalues finally two independent Mathematica programs have been written.

We follow the SUSY Les Houches Accord (SLHA) [38] and compute the parameters M_W^2 and e of our input set defined in Eq. (45) from the SLHA pre-defined input values for the Fermi constant $G_F = 1.16637 \cdot 10^{-5} \text{ GeV}^{-2}$, the Z boson mass $M_Z = 91.187 \text{ GeV}$ and the electroweak coupling $\alpha = 1/137$. If not stated otherwise, we use the running $\overline{\text{DR}}$ top quark mass m_t at a common scale $Q = \sqrt{m_{Q3} m_{tR}}$. It is obtained from the top quark pole mass $M_t = 173.2 \text{ GeV}$ by taking the routines of `NMSSMTools` [39]. In the same way we obtain the running $\overline{\text{DR}}$ bottom quark mass starting from the SLHA input value $m_b(m_b)^{\overline{\text{MS}}} = 4.19 \text{ GeV}$. For the light quarks we chose $m_u = 2.5 \text{ MeV}$, $m_c = 1.27 \text{ GeV}$, $m_d = 4.95 \text{ MeV}$, $m_s = 101 \text{ MeV}$ [40] and for the τ mass $m_\tau = 1.777 \text{ GeV}$.

In the following we exemplify the effects of complex phases in the one-loop corrections to the NMSSM Higgs boson masses in different scenarios. We require the scenarios to be compatible with the recent results of the LHC Higgs boson searches [1, 2] in the limit of the real NMSSM, *i.e.* for vanishing CP-violating phases.¹⁵ Our starting points are the NMSSM benchmark points presented in Ref. [8] which have been slightly modified for our analysis. With not too heavy stop masses and not too substantial mixing they avoid unnaturally large finetuning, and λ and κ have been chosen such that unitarity is not violated below the GUT scale. Furthermore, we paid attention to keep the effective $\mu \leq 200 \text{ GeV}$, with $\mu = \lambda v_s / \sqrt{2}$, in order not to violate tree-level naturalness. For each scenario we verified that the non SM-like Higgs bosons are not excluded by the searches at LEP [27], Tevatron [28] and LHC. This has been cross-checked by running the program `HiggsBounds` [41]¹⁶, which needs the complex NMSSM Higgs couplings and branching ratios. The latter have been obtained by adapting the Fortran code `HDECAY` [46, 47] to the complex NMSSM, in which we use the one-loop corrected Higgs boson masses and mixing matrix elements of our calculation. For the SM-like Higgs boson $H_i^{\text{SM-like}}$ of the real NMSSM we demand its mass to lie in the interval $120 - 130 \text{ GeV}$. Furthermore, the total significance for $H_i^{\text{SM-like}}$ should not deviate by more than 20% from the corresponding SM value. We roughly estimate the significance S to be given by $S = N_s / \sqrt{N_b}$, where N_s denotes the number of signal events and N_b the number of background events. Hence our criteria for a scenario to be compatible with present LHC searches are

$$120 \text{ GeV} \leq M_{H_i^{\text{SM-like}}} \leq 130 \text{ GeV} \quad (109)$$

$$S_{\text{tot}}^{\text{NMSSM}}(H_i^{\text{SM-like}}) = S_{\text{tot}}^{\text{SM}}(H^{\text{SM}}) \pm 20\% \quad \text{for} \quad M_{H^{\text{SM}}} = M_{H_i^{\text{SM-like}}} . \quad (110)$$

In this case the scenario is estimated to be compatible with the present LHC searches taking into account experimental and theoretical uncertainties. We roughly approximate the total significance by adding in quadrature the significances of the various LHC Higgs search channels. We assume the number of background events to be the same both in the SM and the NMSSM case. For the calculation of the signal events we need the cross section values in the different channels,

¹⁵Note, that this is only an arbitrary choice which was made for practical reasons. We could as well have demanded a complex NMSSM scenario to be compatible with the recent LHC searches.

¹⁶The program `NMSSMTools` [39] also performs these checks. It can be used, however, only for the case of the real NMSSM.

which we obtain as follows. We first calculate the inclusive production cross section by adding the gluon fusion, weak boson fusion, Higgs-strahlung and $t\bar{t}$ Higgs production cross sections. Associated production with $b\bar{b}$ does not play a role here, as the $\tan\beta$ values we chose are rather low. The gluon fusion value at NNLO QCD is obtained with `HIGLU` [42], which we have modified to the NMSSM case. Weak boson fusion and Higgs-strahlung at NLO QCD are computed with the programs `VV2H` and `V2HV` [43] by applying the modification factor due to the modified NMSSM Higgs coupling to gauge bosons compared to the SM case. Finally, the cross section value for $t\bar{t}$ Higgs production at NLO QCD [44] is obtained from the cross section values given at the LHC Higgs cross section working group webpage [45] by applying the appropriate factor taking into account the change of the NMSSM Higgs Yukawa coupling with respect to the SM coupling. Note that the NLO QCD corrections are not affected by changes due to the NMSSM Higgs sector and can therefore readily be taken over from the SM case. The cross sections in the WW, ZZ and $\gamma\gamma$ LHC search channels are obtained in the narrow width approximation by multiplication of the total cross section with the corresponding Higgs branching ratios into these final states. The branching ratios have been obtained from our modified Fortran code `HDECAY` [46, 47], adapted to the complex NMSSM. The thus obtained cross sections for the various channels can be used to calculate the number of signal events.¹⁷ The experiments take into account QCD corrections beyond NLO and also electroweak corrections. As these are not available for the NMSSM we cannot take them into account here. They are of the order of a few percent depending on the process. Furthermore, ATLAS and CMS exploit more final states and combine them in a sophisticated statistical procedure, while we have taken into account only the most prominent ones. Our approximation should therefore be viewed only as a rough estimate, good enough though to eliminate scenarios clearly excluded by the present LHC search results.

In all investigated scenarios we have taken the input values at the scale $Q = \sqrt{m_{Q_3} m_{t_R}}$. In order to comply with the present LHC searches [48, 49], we have throughout taken the soft SUSY breaking mass parameters of the squarks of the first two generations equal to 1 TeV, and for simplicity also those of the sleptons. The corresponding trilinear couplings are taken to be 1 TeV. Furthermore, the right-handed soft SUSY breaking mass parameter of the sbottom sector is set equal to 1 TeV and its trilinear coupling close to 1 TeV, so that we have

$$\begin{aligned}
m_U &= m_D = m_{Q_{1,2}} = m_E = m_L = 1 \text{ TeV} \\
A_x &= 1 \text{ TeV} \quad (x = u, c, d, s, e, \mu, \tau) \\
A_b &\approx 1 \text{ TeV} .
\end{aligned}
\tag{111}$$

This leads to masses of ~ 1 TeV for the squarks of the first and second family, the sleptons and the heavier sbottom. Furthermore, all scenarios lead to the correct relic density in the limit of the real NMSSM, which has been checked with `NMSSMTools` which contains a link to `MicrOMEGAs` [50].

¹⁷Note, that the luminosity factor in the calculation of the number of events and also the number of background events drop out in the comparison of the NMSSM case to the SM case, so that we only need to calculate the quadratic sum of the cross sections in the different final states for the NMSSM and for the SM and compare them.

4.1 Scenario with a SM-like H_3

The parameter set for this scenario is given by

$$\begin{aligned}
 |\lambda| = 0.72, \quad |\kappa| = 0.20, \quad \tan \beta = 3, \quad M_{H^\pm} = 629 \text{ GeV}, \quad |A_\kappa| = 27 \text{ GeV}, \quad |\mu| = 198 \text{ GeV} \\
 |A_b| = 963 \text{ GeV}, \quad |A_t| = 875 \text{ GeV}, \quad M_1 = 145 \text{ GeV}, \quad M_2 = 200 \text{ GeV}, \quad M_3 = 600 \text{ GeV}.
 \end{aligned}
 \tag{112}$$

The slightly high values of λ and κ may require extra matter above the TeV scale [8].¹⁸ We set all CP-violating phases to zero and subsequently turn on specific phases to study their respective influence. In this case, the signs of the tree-level CP-violating phases Eqs. (28), (29) are then chosen as

$$\text{sign } \cos \varphi_x = +1, \quad \text{sign } \cos \varphi_z = -1.
 \tag{113}$$

Furthermore, the left- and right-handed soft SUSY breaking mass parameters in the stop sector are given by $m_{Q_3} = 490 \text{ GeV}$ and $m_{t_R} = 477 \text{ GeV}$. This leads to relatively light stop masses $m_{\tilde{t}_1} = 363 \text{ GeV}$ and $m_{\tilde{t}_2} = 616 \text{ GeV}$, still allowed by the experiments [51, 52].¹⁹ In the calculation of the one-loop correction to the Higgs boson masses we have set the renormalization scale equal to 500 GeV, *i.e.* $\mu_{ren} = 500 \text{ GeV}$, if not stated otherwise. This scenario leads in the CP-conserving NMSSM to the one-loop corrected H_3 being SM-like with a mass $M_{H_3} = 125 \text{ GeV}$ compatible with present LHC searches. In the following we discuss for various complex phase choices the phenomenology of the three lightest Higgs bosons. The two heavier ones receive mass corrections of maximally 2 GeV leading to masses of $\sim 642 \text{ GeV}$ so that they are not excluded by present collider searches, with H_4 being mostly CP-odd and H_5 mostly CP-even. We therefore do not display their masses explicitly.

4.1.1 CP violation at tree-level

As we have seen in Sect. 3.1 a non-vanishing phase φ_y , *cf.* Eq. (19), introduces CP violation at tree-level. Therefore CP-even and CP-odd Higgs mass eigenstates cannot be distinguished any more. A measure for CP violation concerning the state H_i ($i = 1, \dots, 5$) is instead provided by the quantity

$$r_{\text{CP}}^i \equiv (\mathcal{R}_{i1})^2 + (\mathcal{R}_{i2})^2 + (\mathcal{R}_{i3})^2,
 \tag{114}$$

where \mathcal{R}_{ij} are the matrix elements of the mixing matrix which diagonalizes the Higgs boson mass matrix, *cf.* Eq. (39). A purely CP-even (CP-odd) mass eigenstate H_i corresponds to $r_{\text{CP}}^i = 1$ (0). We first investigate the effect of a non-vanishing phase²⁰

$$\varphi_\kappa \neq 0.
 \tag{115}$$

The phases $\varphi_{A_\lambda}, \varphi_{A_\kappa}$ are fixed by the tadpole conditions Eqs. (15), (17).

¹⁸Being above the TeV scale it is not expected to influence LHC phenomenology, apart from the indirect effect of allowing λ to be a somewhat larger than allowed by the usual perturbativity requirement in the NMSSM with no extra matter. If instead one accepts more finetuning in the theory and allows for higher stop masses, a Higgs mass of the order of 125 GeV can be achieved for lower λ values, *cf.* the discussion in Sect. 4.2.

¹⁹Note, that light stop masses and small mixing reduce the amount of finetuning [8].

²⁰The choice of non-vanishing φ_κ allows to investigate mixing effects of the Higgs bosons while suppressing the phase relevant for the neutral electric dipole moment [23].

In Fig. 1 (left) we show the tree-level and one-loop masses of the two lightest Higgs mass eigenstates $H_{1,2}$ as a function of φ_κ , where $\varphi_\kappa = 0$ corresponds to the real NMSSM. The phase is varied up to $\pi/8$. Above this value it turns out that the phases φ_{A_λ} and φ_{A_κ} cannot be chosen in such a way that the tadpole conditions are fulfilled. The tree-level and one-loop corrected mass of the SM-like H_3 is shown in Fig. 1 (right). Figure 2 displays, as a function of φ_κ , the amount of CP violation r_{CP}^i (left) and the amount of the CP-even singlet component²¹ $(\mathcal{R}_{i3})^2$ (right) for $H_{1,2,3}$. Finally Fig. 3 shows their coupling squared to the V bosons ($V = Z, W$) normalized to the SM as a function of φ_κ . As expected, the masses exhibit already at tree-level a sensitivity to the CP-violating phase φ_κ . In particular for the SM-like H_3 this dependence is more pronounced at one-loop level, changing its mass value by up to 9 GeV for $\varphi_\kappa \in [0, \pi/8]$. The one-loop correction increases the mass by ~ 4 to 11 GeV depending on φ_κ with larger mass values for larger CP-violating phases.

In the plots the grey areas are the parameter regions which are excluded due to the experimental constraints from LEP, Tevatron and LHC, and which have been obtained with `HiggsBounds`.²² This is the case for $0.074\pi < \varphi_\kappa < 0.099\pi$ and $\varphi_\kappa > 0.112\pi$. The dashed region excludes the parameter regions where the criteria stated in Eq. (110) of compatibility with the recent Higgs excess around 125 GeV cannot be fulfilled any more, here for $\varphi_\kappa > 0.021\pi$. The reason is that with increasing φ_κ the eigenstate H_3 becomes more CP-odd and hence couples less to VV ($V = Z, W$) as can be inferred from Fig. 2 (left) and Fig. 3 so that the total cross section becomes smaller and the significance deviates by more than 20% from the SM significance of a SM Higgs boson with same mass.

The one-loop corrections for the two lighter Higgs bosons $H_{1,2}$ increase their masses by 6-15 GeV depending on φ_κ . The mass value $M_{H_1(H_2)}$ decreases (increases) with rising φ_κ . In the

²¹The CP-odd singlet component is given by $(\mathcal{R}_{i5})^2$.

²²The exclusion is due to the LEP constraint on H_1 from the Higgs boson search in the $Zb\bar{b}$ final state stemming from a Higgs boson produced in Higgs-strahlung with subsequent decay into a b -quark pair.

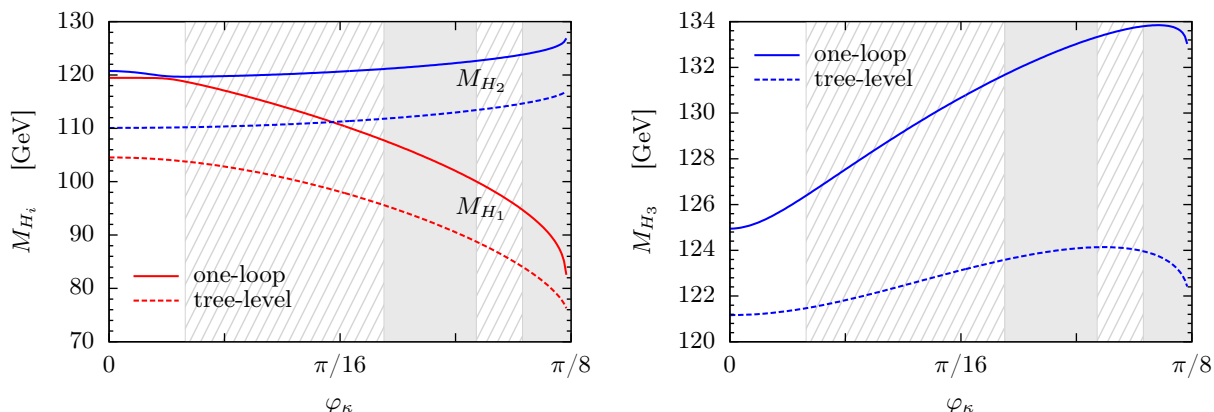


Figure 1: Left: Tree-level (dashed) and one-loop corrected (full) Higgs boson masses for H_1 (red) and H_2 (blue) as a function of φ_κ . Right: Tree-level (dashed) and one-loop (full) mass M_{H_3} as a function of φ_κ . The exclusion region due to LEP, Tevatron and LHC data is shown as grey area, the region with the SM-like Higgs boson not being compatible with an excess of data around 125 GeV as dashed area.

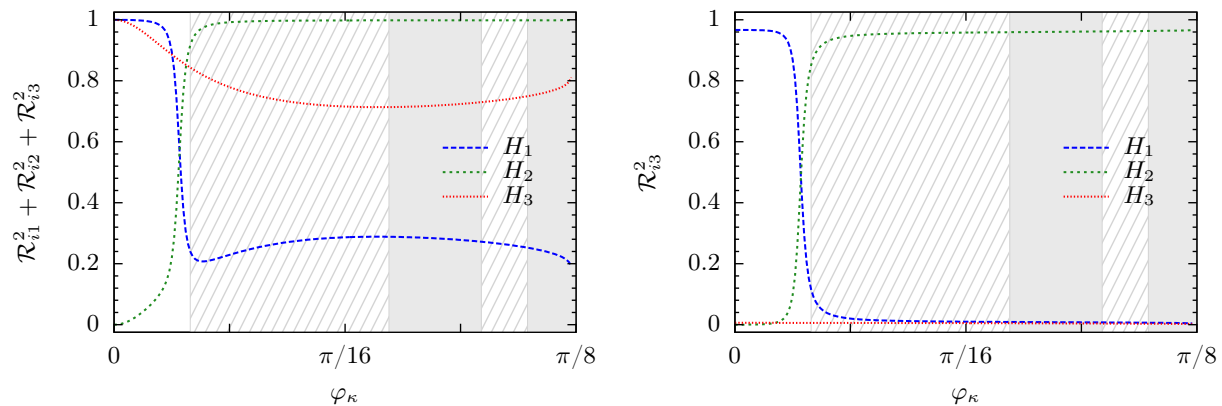


Figure 2: The amount of CP violation r_{CP}^i for H_i ($i = 1, 2, 3$) as a function of φ_κ (left). The amount of CP-even singlet component $(\mathcal{R}_{i3})^2$ as a function of φ_κ (right).

CP-conserving limit the one-loop masses of $H_{1,2}$ are $M_{H_1} = 119.4$ GeV and $M_{H_2} = 120.7$ GeV, with H_1 being CP-even, *cf.* Fig. 2 (left), but CP-even singlet-like, *cf.* Fig. 2 (right), such that it hardly couples to SM particles and cannot be excluded by the experimental searches. The heavier Higgs H_2 is dominantly CP-odd singlet-like (not plotted here) and is not excluded by the LEP, Tevatron and LHC searches due to both its singlet and its CP-odd nature leading to a vanishing coupling to weak vector bosons, *cf.* Fig. 3. With increasing CP-violating phase the eigenstates H_1 and H_2 interchange their roles both with respect to their CP nature and their amount of CP-even singlet component, with the cross-over taking place at $\varphi_\kappa \approx \pi/64$.

In order to get an estimate of the theoretical uncertainty due to the unknown higher-order corrections the one-loop corrections to the Higgs boson masses have been calculated with the top and bottom pole quark masses, $M_t = 173.2$ GeV and $M_b = 4.88$ GeV, and compared to the results for the one-loop corrected masses evaluated with the running $\overline{\text{DR}}$ top and bottom quark masses $m_{t,b}$ at the scale $Q = \sqrt{m_{Q_3} m_{t_R}}$. For our scenario they amount to $m_t = 153.4$ GeV and $m_b = 2.55$ GeV. The result is shown in Fig. 4. Whereas the slope of the curve hardly changes, the

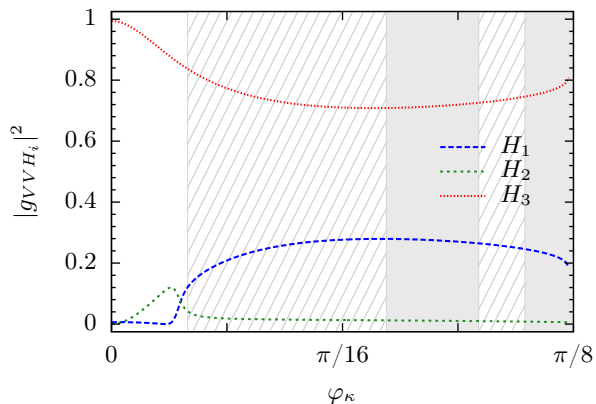


Figure 3: The H_i coupling to V ($V = Z, W$) bosons squared ($i = 1, 2, 3$) normalized to the SM coupling, $|g_{VVH_i}|^2$, as a function of φ_κ .

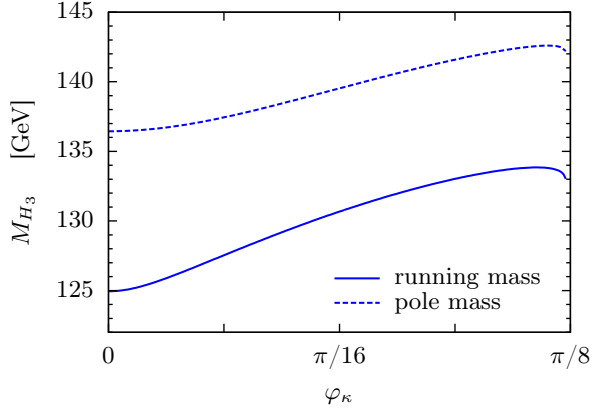


Figure 4: The one-loop corrected mass of the SM-like Higgs H_3 evaluated with the top and bottom running $\overline{\text{DR}}$ masses (full) and with the corresponding pole masses (dashed).

absolute values of the corrections change and are more important for a higher top quark mass. The theoretical uncertainty due to the different quark mass renormalization schemes can conservatively be estimated to $\sim 10\%$.

4.1.2 No tree-level CP violation

We now keep the CP-violating phases φ_κ and φ_λ non-zero and vary them by the same amount, such that according to Eq. (19) we have no tree-level CP-violating phase φ_y . In the one-loop corrections $\varphi_\kappa, \varphi_\lambda$ enter separately so that CP violation is induced radiatively. Figure 5 (left) shows the one-loop corrected masses of the three lightest Higgs states $H_{1,2,3}$, Fig. 5 (right) compares the tree-level and one-loop corrected mass of the SM-like H_3 , both as a function of φ_κ . The tree-level mass shows no dependence on φ_κ as expected. The one-loop mass M_{H_3} changes by only ~ 3 GeV for φ_κ varying from 0 to π , and the loop-corrected masses for $H_{1,2}$ show almost no dependence on the CP-violating phase. The reason is that the dependence on the phase is due to the corrections from the stop sector which are the dominant contributions to the one-loop masses. The values of the

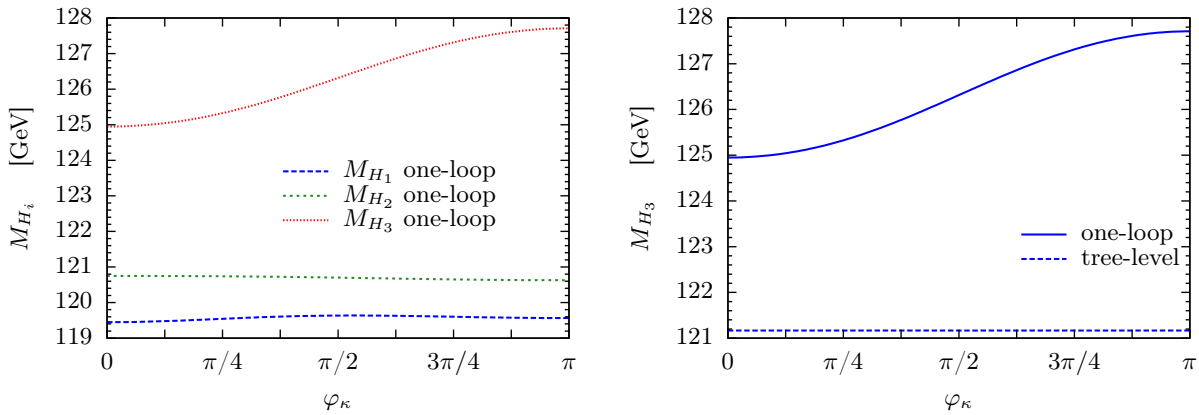


Figure 5: One-loop corrected Higgs boson masses M_{H_i} ($i = 1, 2, 3$) as a function of $\varphi_\kappa = \varphi_\lambda$ (left). Tree-level (dashed) and one-loop corrected (full) mass for H_3 as a function of $\varphi_\kappa = \varphi_\lambda$ (right).

stop masses change with the CP-violating phase. As H_3 has the largest h_u component and hence couples more strongly to the up-type quarks it shows a stronger dependence on φ_κ than H_1 and H_2 . For M_{H_1} (M_{H_2}) the mass corrections are of about 15 (11) GeV. With mass values around 120 GeV they could lead to additional signals at the LHC if they were SM-like. However, due to the CP-odd nature of H_2 , *cf.* Fig. 6 (left), it hardly couples to weak vector bosons. And the CP-even singlet character of H_1 , compare with Fig. 6 (right), reduces its couplings to SM particles. These particles would therefore have considerably reduced signals at the LHC. The whole region over which $\varphi_\kappa = \varphi_\lambda$ are varied is hence still allowed by the LHC searches.

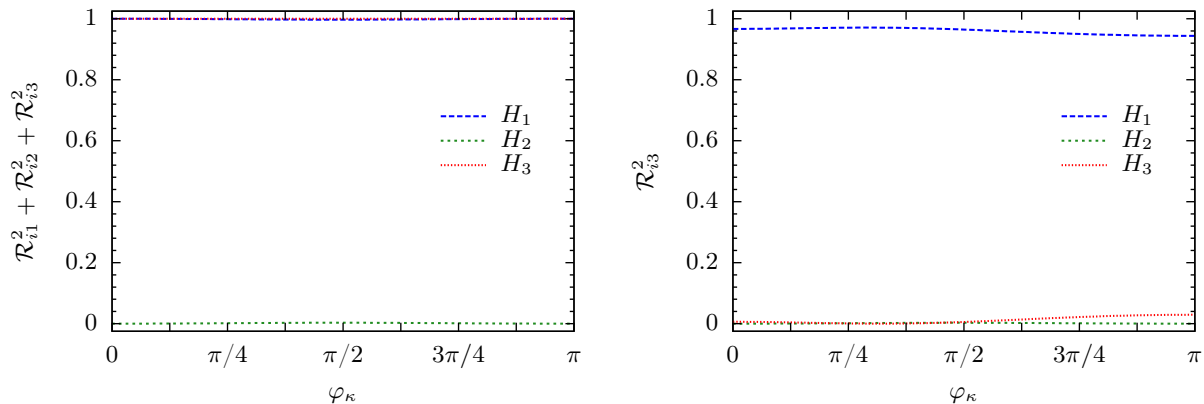


Figure 6: The amount of CP violation r_{CP}^i for H_i ($i = 1, 2, 3$) as a function of $\varphi_\kappa = \varphi_\lambda$ (left). The amount of CP-even singlet component $(\mathcal{R}_{i3})^2$ as a function of $\varphi_\kappa = \varphi_\lambda$ (right).

4.1.3 Radiatively induced CP violation through the stop sector

For completeness we investigate the case where only $\varphi_{A_t} \neq 0$. CP violation is thus only induced through loop corrections stemming from the stop sector. The one-loop corrected masses of $H_{1,2,3}$ are shown in Fig. 7 (left), the tree-level and one-loop corrected mass of the SM-like H_3 are displayed separately in Fig. 7 (right), both as function of φ_{A_t} . The tree-level masses of $H_{1,2}$ are increased by about 10-15 GeV and their one-loop masses of ~ 119.5 and 121 GeV, respectively, hardly show any dependence on φ_{A_t} . The SM-like H_3 one-loop mass shows a small dependence varying by ~ 2 GeV for $\varphi_{A_t} \in [0, \pi]$, increasing the tree-level mass by 4-7 GeV. The reason is that H_3 has the largest h_u component so that the dominant one-loop corrections stemming from the stop loops contribute more importantly to the radiative corrections of the Higgs mass matrix elements of H_3 than of H_1 and H_2 . The CP-even singlet nature of H_1 , the CP-even character of H_1 and H_3 as well as the CP-odd one of H_2 are hardly affected by a change in φ_{A_t} and are therefore not displayed here. As may have been expected, in this scenario loop-induced CP violation affects the phenomenology of the Higgs bosons less. Note, that the scenario is not excluded by LHC searches over the whole displayed phase range.

In Fig. 8 we investigate the theoretical error due to unknown higher-order corrections by varying the renormalization scale from 500 GeV to half and twice the scale. The variation of the renormalization scale also changes the values of the input parameters and the running $\overline{\text{DR}}$ top and bottom mass. For higher scales they become smaller and hence also the one-loop corrections to the masses

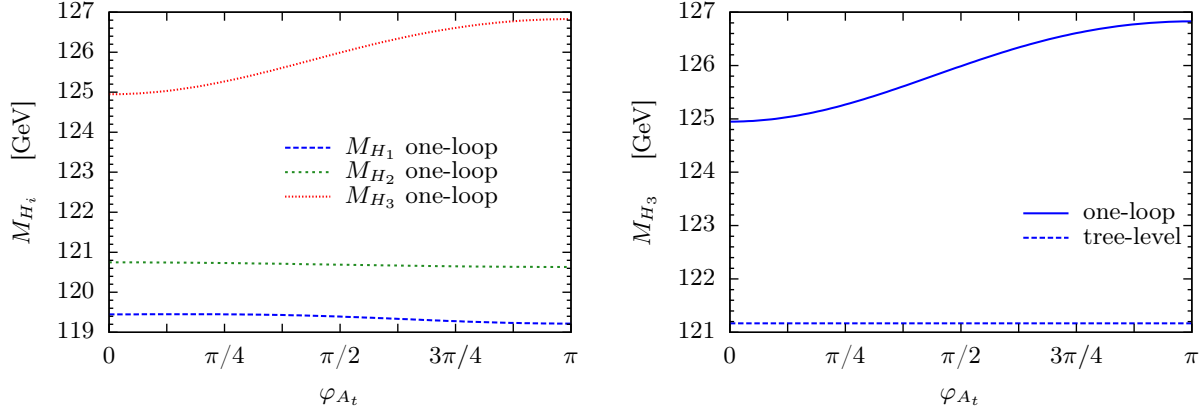


Figure 7: One-loop corrected Higgs boson masses M_{H_i} ($i = 1, 2, 3$) as a function of φ_{A_t} (left). Tree-level (dashed) and one-loop (full) mass M_{H_3} as a function of φ_{A_t} (right).

decrease. The residual theoretical uncertainty can be estimated to about 4%. We also checked the theoretical uncertainty due to the different quark mass renormalization schemes and found them to be of $\sim 10\%$, hence of the same order as in the scenario studied in Sect. 4.1.

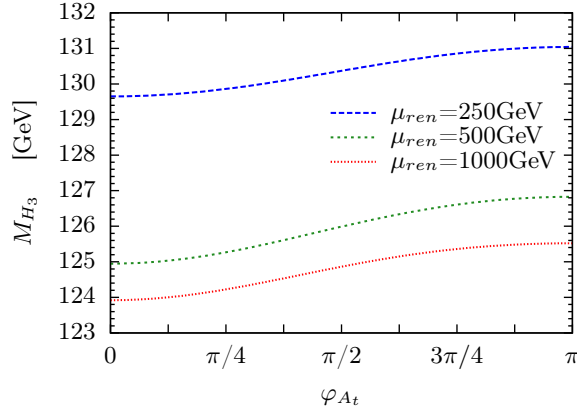


Figure 8: One-loop corrected Higgs boson masses M_{H_3} as a function of φ_{A_t} for three different renormalization scales, $\mu_{ren} = 250$ (blue/long-dashed), 500 (green/short-dashed) and 1000 GeV (red/dotted).

In summary, the discussion of the various scenarios has shown that the impact of the CP-violating phase is crucial for the validity of the model. While a certain parameter set can still accommodate the experimental results for vanishing CP violation it may be invalidated by non-vanishing CP phases. Turning this around, the experimental results will be useful to pin down the allowed amount of CP violation. The latter can arise from tree-level CP-violating phases in the Higgs sector or be radiatively induced. In the latter case the effects are found to be less pronounced. To get reliable predictions, the one-loop corrections have to be included as they not only considerably change the absolute mass values but also the singlet and CP-nature of the individual Higgs bosons as compared to the tree-level quantities.

4.2 Scenario with SM-like H_1 or H_2

The parameter set for this scenario, where, depending on the CP-violating phase, either H_1 or H_2 is SM-like, is given by

$$|\lambda| = 0.65, \quad |\kappa| = 0.25, \quad \tan \beta = 3, \quad M_{H^\pm} = 619 \text{ GeV}, \quad |A_\kappa| = 18 \text{ GeV}, \quad |\mu| = 199 \text{ GeV} \\ |A_b| = 971 \text{ GeV}, \quad |A_t| = 1143 \text{ GeV}, \quad M_1 = 105 \text{ GeV}, \quad M_2 = 200 \text{ GeV}, \quad M_3 = 600 \text{ GeV}. \quad (116)$$

The signs of the tree-level CP-violating phases Eqs. (28) and (29) are

$$\text{sign } \cos \varphi_x = +1, \quad \text{sign } \cos \varphi_z = -1. \quad (117)$$

The renormalization scale has been set to $\mu_{ren} = 650 \text{ GeV}$. The left- and right-handed soft SUSY breaking mass parameters in the stop sector $m_{Q_3} = 642 \text{ GeV}$ and $m_{t_R} = 632 \text{ GeV}$ lead to $m_{\tilde{t}_1} = 514 \text{ GeV}$ and $m_{\tilde{t}_2} = 768 \text{ GeV}$. The low value of λ respects the bounds imposed by unitarity [8]. We allow for tree-level CP violation by choosing $\varphi_\kappa \neq 0$. The remaining complex phases are all set to zero, except for φ_{A_λ} and φ_{A_κ} which follow from the tadpole conditions Eqs. (15), (17).

The tree-level and one-loop corrected masses of H_1 and H_2 are shown in Fig. 9 (left), as a function of φ_κ . Beyond $\varphi_\kappa \approx 0.1\pi$ the tadpole conditions are not fulfilled any more. The corresponding couplings squared to weak vector bosons are plotted in Fig. 9 (right). The amount of CP violation of the three lightest Higgs bosons $H_{1,2,3}$ and their CP-even singlet component are displayed in Fig. 10 (left) and (right), respectively, as a function of φ_κ . As can be inferred from the Figures, in the limit of the real NMSSM H_1 is CP-even and has SM-like couplings while H_2 is CP-odd. The heavier H_3 is CP-even over the whole φ_κ range. The CP-even singlet components of H_1 and H_2 vanish, *cf.* Fig. 10 (right). However, H_2 is CP-odd singlet-like. This is reflected in the couplings of H_1 and H_2 to the weak vector bosons. The one-loop corrections for $\varphi_\kappa = 0$ shift the H_1 mass from 99 to about 122 GeV so that its mass is compatible with the excess observed

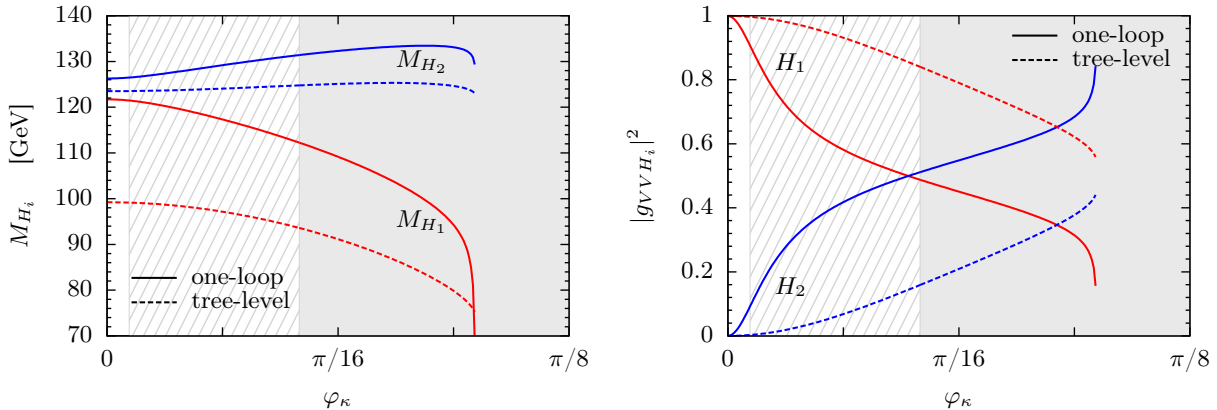


Figure 9: Left: Tree-level (dashed) and one-loop corrected (full) Higgs boson masses as a function of φ_κ for H_1 (red) and H_2 (blue). Right: The H_1 (red) and H_2 (blue) Higgs couplings squared to two V bosons ($V = W, Z$) as a function of φ_κ at tree-level (dashed) and at one-loop (full). The exclusion region due to LEP, Tevatron and LHC data is shown as grey area, the region with the SM-like Higgs boson not being compatible with an excess of data around 125 GeV as dashed area.

at the LHC. The mass of the second Higgs boson H_2 is increased by about 3 GeV to 126 GeV and could have been observed at the LHC, if its coupling to gauge bosons were not suppressed due to its CP-odd character so that it is not excluded by the present experimental constraints from the LHC. Furthermore, for $\varphi_\kappa = 0$ the total significance concerning H_1 is compatible with LHC searches according to our criteria Eq. (110).

The scenario is interesting because with increasing φ_κ the CP character of $H_{1,2}$ changes rapidly (with a cross-over at $\varphi_\kappa \approx 3\pi/64$ where $H_{1,2}$ interchange their roles with H_1 being more CP-odd like and H_2 more CP-even like). This dependence on the CP violating phase is at one-loop more pronounced than at tree-level and makes that already beyond $\varphi_\kappa \approx 0.006\pi$ H_1 cannot fulfill the role of the SM-like Higgs boson any more as its couplings deviate too much from the SM case to fulfill the requirement of Eq. (110). On the other hand, the H_2 couplings are not yet SM-like and once this is the case H_2 is already too heavy to be compatible with LHC searches. Hence, above $\varphi_\kappa \approx 0.006\pi$ the scenario does not comply with the criteria of Eq. (110) any more and it is excluded as indicated by the dashed region. Beyond $\varphi_\kappa \approx 0.052\pi$ the grey region shows that the searches at LEP invalidate this parameter choice due to the LEP limit on H_1 in $Zb\bar{b}$. Therefore a large portion of this scenario is likely to be excluded, constraining φ_κ to be almost zero and hence a real NMSSM.

This scenario illustrates particularly well the importance of the one-loop corrections and the impact on the restriction of a possible CP-violating phase. Firstly, the one-loop corrections are crucial to shift the mass of the SM-like Higgs boson to a mass value which is compatible with the excess observed at the LHC. However, the one-loop corrections also amplify the dependence on the CP-violating phase of both the Higgs masses and in particular the mixing matrix elements and hence the coupling to the weak vector bosons. Neglecting for the moment for the sake of this discussion the fact that at tree-level H_1 does not fulfill the mass constraint, the restriction of the CP-violating phase due to deviations from the SM significance would be less severe at tree-level than at one-loop level due to the smooth tree-level dependence on the CP-violating phase. The one-loop corrections are hence crucial to correctly define parameter scenarios which are compatible with present LHC searches and to derive the correct exclusion limits for scenarios dropping out of

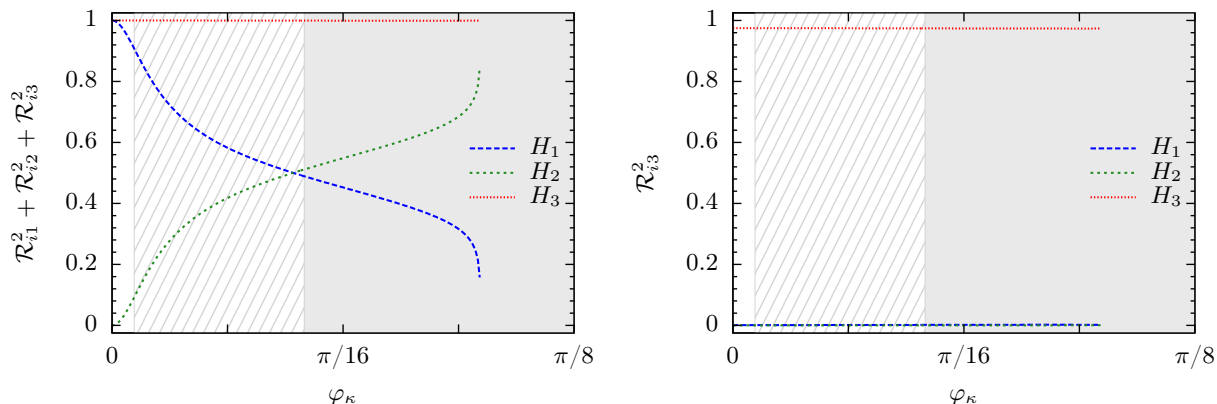


Figure 10: The amount of CP violation r_{CP}^i for H_i ($i = 1, 2, 3$) as a function of φ_κ (left). The amount of CP-even singlet component $(\mathcal{R}_{i3})^2$ as a function of φ_κ (right).

this constraint.

We close this subsection with the discussion of the CP-even H_3 , not shown explicitly in all plots. It is dominantly CP-even singlet-like. Its tree-level mass of $\sim 148 - 152$ GeV for φ_κ increasing from 0 to $\sim 3\pi/16$ receives one-loop corrections of $\sim 3 - 4$ GeV. The one-loop corrections show the same dependence on φ_κ as the tree-level mass. Due to its singlet character at present it cannot be excluded by LHC searches.

5 Summary and Conclusions

We have calculated the one-loop corrections to the neutral Higgs bosons in the CP-violating NMSSM by applying a mixed renormalization scheme where part of the parameters are renormalized on-shell while $\tan\beta, v_s, \lambda, \kappa, A_\kappa$ and the CP-violating phases are renormalized in the $\overline{\text{DR}}$ scheme. We have in general allowed for tree-level CP violation due to non-vanishing phases $\varphi_u, \varphi_s, \varphi_\kappa$ and φ_λ , and for loop induced CP violation from the stop sector due to a non-zero phase φ_{A_t} . Several scenarios have been investigated which start from parameter sets that are compatible with the experimental Higgs searches in the limit of the real NMSSM, subsequently CP violation is turned on. As expected the dependence of the one-loop corrected Higgs masses and mixing matrix elements on the CP-violating phase turned out to be more pronounced for tree-level CP violation than for radiatively induced CP violation. The loop corrections were found to considerably change the masses and mixing angles with crucial implications for the Higgs phenomenology at the LHC. As it is well known in the MSSM and the real NMSSM we also found that a scenario may be excluded at tree-level, whereas it is compatible with LHC searches at one-loop. Of special interest is the dependence on the CP-violating phase. It may be rather smooth at tree-level but more pronounced at one-loop so that at one-loop the CP-violating phase under investigation may be much more restricted than at tree-level due to possible non-compatibility with the experiments. Therefore, in order to correctly define viable scenarios and pin down allowed parameter ranges the one-loop corrections are indispensable. We also investigated the theoretical error due to the unknown higher order corrections by applying an on-shell and a $\overline{\text{DR}}$ renormalization scheme for the top and bottom quark mass and by varying the renormalization scale between half and twice its value. The theoretical error of the one-loop corrected Higgs masses can be conservatively estimated to be about 10%.

Acknowledgments

We would like to thank J. Baglio, M. Maniatis, M. Spira and D. Stöckinger for helpful discussions. This research was supported in part by the Deutsche Forschungsgemeinschaft via the Sonderforschungsbereich/Transregio SFB/TR-9 Computational Particle Physics. R.G. acknowledges financial support from the Landesgraduiertenkolleg.

A Relations between Original and Physical Parameters

For the transformation of the Lagrangian from the original parameters to the physical ones the following relations are used:

$$m_{H_d}^2 = \frac{e}{2c_\beta M_W s_{\theta_W}} t_{h_d} - \left[\frac{M_Z^2 c_{2\beta}}{2} - v_s t_\beta |\lambda| \left(\frac{|A_\lambda|}{\sqrt{2}} c_{\varphi_x} + |\kappa| \frac{v_s}{2} c_{\varphi_y} \right) + |\lambda|^2 \left(\frac{2s_\beta^2 M_W^2 s_{\theta_W}^2}{e^2} + \frac{v_s^2}{2} \right) \right], \quad (118)$$

$$m_{H_u}^2 = \frac{e}{2s_\beta M_W s_{\theta_W}} t_{h_u} + \left[\frac{M_Z^2 c_{2\beta}}{2} + \frac{|\lambda| v_s}{t_\beta} \left(\frac{|A_\lambda|}{\sqrt{2}} c_{\varphi_x} + |\kappa| \frac{v_s}{2} c_{\varphi_y} \right) - |\lambda|^2 \left(\frac{2c_\beta^2 M_W^2 s_{\theta_W}^2}{e^2} + \frac{v_s^2}{2} \right) \right], \quad (119)$$

$$m_S^2 = \frac{t_{h_s}}{v_s} + \left[s_{2\beta} |\lambda| \left(\frac{|A_\lambda|}{\sqrt{2}} c_{\varphi_x} + |\kappa| v_s c_{\varphi_y} \right) - |\lambda|^2 v_s \right] \frac{2M_W^2 s_{\theta_W}^2}{e^2 v_s} - |\kappa|^2 v_s^2 - \frac{1}{\sqrt{2}} |A_\kappa| |\kappa| v_s c_{\varphi_z}, \quad (120)$$

$$\varphi_{A_\lambda} = \text{sign}_x \left[n_x(\pi) + (-1)^{n_x} \left| \arcsin \left(\frac{e}{\sqrt{2} |A_\lambda| M_W s_{\theta_W} s_\beta |\lambda| v_s} t_{a_d} + \frac{|\kappa| v_s}{\sqrt{2} |A_\lambda|} s_{\varphi_y} \right) \right| \right] - \varphi_\lambda - \varphi_s - \varphi_u, \quad (121)$$

$$\varphi_{A_\kappa} = \text{sign}_z \left[n_z(\pi) + (-1)^{n_z} \left| \arcsin \left(\frac{\sqrt{2}}{|A_\kappa| v_s} \left[\frac{2M_W s_{\theta_W} c_\beta}{e |\kappa| v_s^2} t_{a_d} + \frac{3M_W^2 s_{\theta_W}^2 s_{2\beta} |\lambda|}{e^2} s_{\varphi_y} - \frac{1}{|\kappa| v_s} t_{a_s} \right] \right) \right| \right] - \varphi_\kappa - 3\varphi_s, \quad (122)$$

$$|A_\lambda| = \frac{s_{2\beta}}{\sqrt{2} c_{\varphi_x} |\lambda| v_s c_{\Delta\beta}^2} \left[M_{H^\pm}^2 - M_W^2 c_{\Delta\beta}^2 - |\kappa| |\lambda| v_s^2 \frac{c_{\Delta\beta}^2}{s_{2\beta}} c_{\varphi_y} + \frac{2M_W^2 s_{\theta_W}^2 c_{\Delta\beta}^2}{e^2} |\lambda|^2 - \frac{e}{2M_W s_{\theta_W}} \left[t_{h_u} \frac{c_{\beta_c}^2}{s_\beta} + t_{h_d} \frac{s_{\beta_c}^2}{c_\beta} \right] \right], \quad (123)$$

$$v_u = \frac{2M_W s_{\theta_W} s_\beta}{e}, \quad v_d = \frac{2M_W s_{\theta_W} c_\beta}{e}, \quad (124)$$

$$g = \frac{e}{s_{\theta_W}}, \quad g' = \frac{e}{c_{\theta_W}} \quad \text{with} \quad c_{\theta_W} = \frac{M_W}{M_Z} \quad \text{and} \quad s_{\theta_W}^2 = 1 - c_{\theta_W}^2, \quad (125)$$

where n_x and n_z can be zero or one in case of two solutions of the tadpole condition, Eqs. (15) and (17), and zero if there exists only a single one. Here, sign_x and sign_z are the sign of the corresponding arcsine evaluated in the interval $[-\pi, \pi)$, respectively.

B Higgs Boson Mass Matrix

In this section we list the Higgs boson mass matrix elements in a form needed as starting point for the renormalization procedure in the basis $\Phi = (h_d, h_u, h_s, A, a_s, G)^T$. This basis is obtained by transforming the original basis $\phi = (h_d, h_u, h_s, a_u, a_d, a_s)^T$ with the matrix

$$\mathcal{R}^G = \begin{pmatrix} \mathbb{1} & 0 \\ 0 & \mathcal{U}^G \end{pmatrix} \quad \text{and} \quad \mathcal{U}^G = \begin{pmatrix} s_{\beta_n} & c_{\beta_n} & 0 \\ 0 & 0 & 1 \\ c_{\beta_n} & -s_{\beta_n} & 0 \end{pmatrix}. \quad (126)$$

The angle β_n is chosen such that the Goldstone boson field (with zero mass eigenvalue) is extracted and, at tree-level, coincides with the angle β defined via the ratio of the vacuum expectation values, $\beta_n = \beta$.

The mass matrix elements of the CP-even part M_{hh} , *cf.* Eq. (21), are

$$M_{h_d h_d} = \left[\frac{M_{H^\pm}^2}{c_{\Delta\beta}^2} - M_W^2 \right] s_\beta^2 + M_Z^2 c_\beta^2 + \frac{ec_\beta c_{\beta_B}^2}{2M_W s_{\theta_W} c_{\Delta\beta}^2} [(1 + 2t_\beta t_{\beta_B}) t_{h_d} - t_\beta t_{h_u}] \\ + 2|\lambda|^2 M_W^2 \frac{s_{\theta_W}^2}{e^2} s_\beta^2, \quad (127)$$

$$M_{h_d h_u} = - \left[\frac{M_{H^\pm}^2}{c_{\Delta\beta}^2} - M_W^2 + M_Z^2 \right] s_\beta c_\beta + \frac{ec_\beta c_{\beta_B}^2}{2M_W s_{\theta_W} c_{\Delta\beta}^2} [t_{h_u} + t_\beta t_{\beta_B}^2 t_{h_d}] \\ + |\lambda|^2 M_W^2 \frac{s_{\theta_W}^2}{e^2} s_{2\beta}, \quad (128)$$

$$M_{h_u h_u} = \left[\frac{M_{H^\pm}^2}{c_{\Delta\beta}^2} - M_W^2 \right] c_\beta^2 + M_Z^2 s_\beta^2 + \frac{ec_\beta s_{2\beta_B}}{4M_W s_{\theta_W} c_{\Delta\beta}^2} [(2 + t_\beta t_{\beta_B}) t_{h_u} - t_{\beta_B} t_{h_d}] \\ + 2|\lambda|^2 M_W^2 \frac{s_{\theta_W}^2}{e^2} c_\beta^2, \quad (129)$$

$$M_{h_d h_s} = - \left[\frac{M_{H^\pm}^2}{c_{\Delta\beta}^2} - M_W^2 \right] \frac{M_W s_{\theta_W} s_\beta s_{2\beta}}{e v_s} + \frac{s_\beta c_\beta c_{\beta_B}^2}{v_s c_{\Delta\beta}^2} [t_{h_u} + t_\beta t_{\beta_B}^2 t_{h_d}] \\ + |\lambda| M_W \frac{s_{\theta_W}}{e} v_s [2|\lambda| c_\beta - |\kappa| s_\beta c_{\varphi_y}] - \frac{4|\lambda|^2 M_W^3 s_{\theta_W}^3 s_\beta^2 c_\beta}{e^3 v_s}, \quad (130)$$

$$M_{h_u h_s} = - \left[\frac{M_{H^\pm}^2}{c_{\Delta\beta}^2} - M_W^2 \right] \frac{M_W s_{\theta_W} c_\beta s_{2\beta}}{e v_s} + \frac{c_\beta^2 c_{\beta_B}^2}{v_s c_{\Delta\beta}^2} [t_{h_u} + t_\beta t_{\beta_B}^2 t_{h_d}] \\ + |\lambda| M_W \frac{s_{\theta_W}}{e} v_s [2|\lambda| s_\beta - |\kappa| c_\beta c_{\varphi_y}] - \frac{4|\lambda|^2 M_W^3 s_{\theta_W}^3 s_\beta c_\beta^2}{e^3 v_s}, \quad (131)$$

$$M_{h_s h_s} = \left[\frac{M_{H^\pm}^2}{c_{\Delta\beta}^2} - M_W^2 \right] \frac{M_W^2 s_{\theta_W}^2 s_{2\beta}^2}{e^2 v_s^2} - \frac{M_W s_{\theta_W} s_{2\beta} c_\beta c_{\beta_B}^2}{e v_s^2 c_{\Delta\beta}^2} [t_{h_u} + t_\beta t_{\beta_B}^2 t_{h_d}] + \frac{t_{h_s}}{v_s} \\ + |\lambda| M_W^2 \frac{s_{\theta_W}^2 s_{2\beta}}{e^2 v_s^2} [2|\lambda| M_W^2 \frac{s_{\theta_W}^2}{e^2} s_{2\beta} - |\kappa| v_s^2 c_{\varphi_y}] + 2|\kappa|^2 v_s^2 + \frac{1}{\sqrt{2}} |A_\kappa| |\kappa| v_s c_{\varphi_z}, \quad (132)$$

where $\Delta\beta = \beta - \beta_B$ and $\beta_B \equiv \beta_c = \beta_n$. The mixing angle of the charged Higgs bosons, β_c , and the mixing angle β_n , needed for extracting the Goldstone boson, coincide and no discrimination between these two mixing angles is done in the formulae. The angles φ_x , φ_y and φ_z have been defined in Eqs. (18)–(20).

The mass matrix elements corresponding to the CP-odd components of the Higgs boson mass matrix are given as

$$M_{AA} = M_{H^\pm}^2 - M_W^2 c_{\Delta\beta}^2 + 2|\lambda|^2 M_W^2 \frac{s_{\theta_W}^2}{e^2} c_{\Delta\beta}^2, \quad (133)$$

$$M_{Aa_s} = [M_{H^\pm}^2 - M_W^2 c_{\Delta\beta}^2] \frac{M_W s_{\theta_W} s_{2\beta}}{e v_s c_{\Delta\beta}} - \frac{c_\beta c_{\beta_B}^2}{v_s c_{\Delta\beta}} [t_{h_u} + t_\beta t_{\beta_B}^2 t_{h_d}] \\ + |\lambda| M_W \frac{s_{\theta_W} c_{\Delta\beta}}{e v_s} [2|\lambda| M_W^2 \frac{s_{\theta_W}^2}{e^2} s_{2\beta} - 3|\kappa| v_s^2 c_{\varphi_y}], \quad (134)$$

$$\begin{aligned}
M_{a_s a_s} = & [M_{H^\pm}^2 - M_W^2 c_{\Delta\beta}^2] \frac{M_W^2 s_{\theta_W}^2 s_{2\beta}^2}{e^2 v_s^2 c_{\Delta\beta}^2} - \frac{M_W s_{\theta_W} s_{2\beta} c_\beta c_{\beta_B}^2}{e v_s^2 c_{\Delta\beta}^2} [t_{h_u} + t_\beta t_{\beta_B}^2 t_{h_d}] + \frac{t_{h_s}}{v_s} \\
& + |\lambda| M_W^2 \frac{s_{\theta_W}^2 s_{2\beta}}{e^2 v_s^2} [2|\lambda| M_W^2 \frac{s_{\theta_W}^2}{e^2} s_{2\beta} + 3|\kappa| v_s^2 c_{\varphi_y}] - \frac{3}{\sqrt{2}} |A_\kappa| |\kappa| v_s c_{\varphi_z} , \tag{135}
\end{aligned}$$

$$M_{AG} = [M_{H^\pm}^2 - M_W^2 c_{\Delta\beta}^2] t_{\Delta\beta} + \frac{e c_{\beta_B}}{2 M_W s_{\theta_W} c_{\Delta\beta}} [t_{\beta_B} t_{h_d} - t_{h_u}] + |\lambda|^2 M_W^2 \frac{s_{\theta_W}^2}{e^2} s_{2\Delta\beta} , \tag{136}$$

$$\begin{aligned}
M_{a_s G} = & [M_{H^\pm}^2 - M_W^2 c_{\Delta\beta}^2] \frac{M_W s_{\theta_W} s_{2\beta} s_{\Delta\beta}}{e v_s c_{\Delta\beta}^2} - \frac{c_\beta c_{\beta_B}^2 s_{\Delta\beta}}{v_s c_{\Delta\beta}^2} [t_{h_u} + t_\beta t_{\beta_B}^2 t_{h_d}] \\
& + |\lambda| M_W \frac{s_{\theta_W} s_{\Delta\beta}}{e v_s} [2|\lambda| M_W^2 \frac{s_{\theta_W}^2}{e^2} s_{2\beta} - 3|\kappa| v_s^2 c_{\varphi_y}] , \tag{137}
\end{aligned}$$

$$M_{GG} = [M_{H^\pm}^2 - M_W^2 c_{\Delta\beta}^2] t_{\Delta\beta}^2 + \frac{e c_{\beta-2\beta_B}}{2 M_W s_{\theta_W} c_{\Delta\beta}^2} [t_{h_d} - t_{\beta-2\beta_B} t_{h_u}] + 2|\lambda|^2 M_W^2 \frac{s_{\theta_W}^2}{e^2} s_{\Delta\beta}^2 . \tag{138}$$

Finally, the mass matrix elements describing the mixing between the CP-even and the CP-odd components can be expressed as

$$M_{ha} \mathcal{M}^{\mathcal{G}T} = \begin{pmatrix} \frac{e c_{\beta_B}}{2 M_W s_{\theta_W} s_\beta} t_{a_d} & \frac{1}{v_s} t_{a_d} + 3|\kappa| |\lambda| M_W \frac{s_{\theta_W}}{e} v_s s_\beta s_{\varphi_y} & -\frac{e s_{\beta_B}}{2 M_W s_{\theta_W} s_\beta} t_{a_d} \\ \frac{e s_{\beta_B}}{2 M_W s_{\theta_W} s_\beta} t_{a_d} & \frac{1}{v_s t_\beta} t_{a_d} + 3|\kappa| |\lambda| M_W \frac{s_{\theta_W}}{e} v_s c_\beta s_{\varphi_y} & \frac{e c_{\beta_B}}{2 M_W s_{\theta_W} s_\beta} t_{a_d} \\ M_{h_s A} & M_{h_s a_s} & M_{h_s G} \end{pmatrix} \tag{139}$$

with

$$M_{h_s A} = \frac{c_{\Delta\beta}}{v_s s_\beta} t_{a_d} - |\kappa| |\lambda| M_W \frac{s_{\theta_W}}{e} v_s c_{\Delta\beta} s_{\varphi_y} , \tag{140}$$

$$M_{h_s a_s} = \frac{2}{v_s} t_{a_s} - \frac{4 M_W s_{\theta_W}}{e} \left[\frac{c_\beta}{v_s^2} t_{a_d} + |\kappa| |\lambda| M_W \frac{s_{\theta_W}}{e} s_{2\beta} s_{\varphi_y} \right] , \tag{141}$$

$$M_{h_s G} = \frac{s_{\Delta\beta}}{v_s s_\beta} t_{a_d} - |\kappa| |\lambda| M_W \frac{s_{\theta_W}}{e} v_s s_{\Delta\beta} s_{\varphi_y} . \tag{142}$$

C Chargino and Neutralino Self-Energies

In this section the expressions for the renormalized self-energies of the charginos and neutralinos are listed. The different parts of the renormalized chargino self-energy decomposed according to Eq. (73) can be written as ($i, j=1,2$)

$$[\hat{\Sigma}_{\chi^+}^R(p^2)]_{ij} = [\Sigma_{\chi^+}^R(p^2)]_{ij} + \frac{1}{2} [U^* (\delta Z_R^C + \delta Z_R^{C*}) U^T]_{ij} , \tag{143}$$

$$[\hat{\Sigma}_{\chi^+}^L(p^2)]_{ij} = [\Sigma_{\chi^+}^L(p^2)]_{ij} + \frac{1}{2} [V (\delta Z_L^C + \delta Z_L^{C*}) V^\dagger]_{ij} , \tag{144}$$

$$[\hat{\Sigma}_{\chi^+}^{Ls}(p^2)]_{ij} = [\Sigma_{\chi^+}^{Ls}(p^2)]_{ij} - \frac{1}{2} m_{\chi_k^\pm} ([U^* \delta Z_R^C U^T]_{ik} \delta_{kj} + \delta_{ik} [V \delta Z_L^C V^\dagger]_{kj}) - [U^* \delta M_C V^\dagger]_{ij} , \tag{145}$$

$$[\hat{\Sigma}_{\chi^+}^{Rs}(p^2)]_{ij} = [\Sigma_{\chi^+}^{Rs}(p^2)]_{ij} - \frac{1}{2} m_{\chi_k^\pm} ([V \delta Z_L^{C*} V^\dagger]_{ik} \delta_{kj} + \delta_{ik} [U^* \delta Z_R^{C*} U^T]_{kj}) - [V \delta M_C^\dagger U^T]_{ij} , \tag{146}$$

where, for the renormalization procedure, the chargino spinors as given in Eq. (8) and the 2×2 chargino mass matrix M_C are replaced by

$$\psi_L^+ \rightarrow \left(\mathbb{1} + \frac{1}{2} \delta Z_L^C \right) \psi_L^+ , \quad (147)$$

$$\psi_R^- \rightarrow \left(\mathbb{1} + \frac{1}{2} \delta Z_R^C \right) \psi_R^- , \quad \text{with} \quad \delta Z_X^C = \begin{pmatrix} \delta Z_{X_1}^C & 0 \\ 0 & \delta Z_{X_2}^C \end{pmatrix} \quad \text{and} \quad X = L, R , \quad (148)$$

and

$$M_C \rightarrow M_C + \delta M_C , \quad (149)$$

respectively, where δM_C is given in Eq. (78).

The various parts of the decomposed renormalized neutralino self-energy can be expressed as ($i, j=1, \dots, 5$)

$$[\hat{\Sigma}_{\chi^0}^R(p^2)]_{ij} = [\Sigma_{\chi^0}^R(p^2)]_{ij} + \frac{1}{2} [\mathcal{N}^* (\delta Z^N + \delta Z^{N*}) \mathcal{N}^T]_{ij} , \quad (150)$$

$$[\hat{\Sigma}_{\chi^0}^L(p^2)]_{ij} = [\Sigma_{\chi^0}^L(p^2)]_{ij} + \frac{1}{2} [\mathcal{N} (\delta Z^N + \delta Z^{N*}) \mathcal{N}^\dagger]_{ij} , \quad (151)$$

$$\begin{aligned} [\hat{\Sigma}_{\chi^0}^{Ls}(p^2)]_{ij} &= [\Sigma_{\chi^0}^{Ls}(p^2)]_{ij} - \frac{1}{2} m_{\chi_k^0} ([\mathcal{N}^* \delta Z^N \mathcal{N}^\dagger]_{ik} \delta_{kj} + \delta_{ik} [\mathcal{N}^* \delta Z^N \mathcal{N}^\dagger]_{kj}) \\ &\quad - [\mathcal{N}^* \delta M_N \mathcal{N}^\dagger]_{ij} , \end{aligned} \quad (152)$$

$$\begin{aligned} [\hat{\Sigma}_{\chi^0}^{Rs}(p^2)]_{ij} &= [\Sigma_{\chi^0}^{Rs}(p^2)]_{ij} - \frac{1}{2} m_{\chi_k^0} ([\mathcal{N} \delta Z^{N*} \mathcal{N}^T]_{ik} \delta_{jk} + \delta_{ik} [\mathcal{N} \delta Z^{N*} \mathcal{N}^T]_{kj}) \\ &\quad - [\mathcal{N} \delta M_N^\dagger \mathcal{N}^T]_{ij} . \end{aligned} \quad (153)$$

For the renormalization procedure, the neutralino spinor defined in Eq. (7) has been replaced by

$$\psi^0 \rightarrow \left(\mathbb{1} + \frac{1}{2} \delta Z^N \right) \psi^0 \quad \text{with} \quad \delta Z^N = \text{diag}(\delta Z_1^N, \delta Z_2^N, \delta Z_3^N, \delta Z_4^N, \delta Z_5^N) \quad (154)$$

and the neutralino mass matrix by

$$M_N \rightarrow M_N + \delta M_N . \quad (155)$$

The matrix elements of δM_N can be found in Eqs. (86)–(96).

References

- [1] S. Chatrchyan *et al.* [CMS Collaboration], arXiv:1202.1416 [hep-ex], arXiv:1202.1487 [hep-ex], arXiv:1202.1488 [hep-ex], arXiv:1202.1489 [hep-ex], arXiv:1202.1997 [hep-ex], arXiv:1202.3478 [hep-ex], arXiv:1202.3617 [hep-ex], arXiv:1202.4083 [hep-ex] and arXiv:1202.4195 [hep-ex].
- [2] G. Aad *et al.* [ATLAS Collaboration], Phys. Lett. B **710** (2012) 49 [arXiv:1202.1408 [hep-ex]], Phys. Rev. Lett. **108**, 111803 (2012) [arXiv:1202.1414 [hep-ex]], Phys. Lett. B **710** (2012) 383 [arXiv:1202.1415 [hep-ex]], arXiv:1206.0756 [hep-ex], arXiv:1206.2443 [hep-ex], arXiv:1206.5971 [hep-ex], arXiv:1206.6074 [hep-ex] and arXiv:1205.6744 [hep-ex].

- [3] D.V. Volkov and V.P. Alkulo, Phys. Lett. **B46** (1973) 109; J. Wess and B. Zumino, Nucl. Phys. **B70** (1974) 39; P. Fayet, Phys. Lett. **B64** (1976) 159, Phys. Lett. **B69** (1977) 489, Phys. Lett. **B84** (1979) 416; G.F. Farrar and P. Fayet, Phys. Lett. **B76** (1978) 575; S. Dimopoulos and H. Georgi, Nucl. Phys. **B193** (1981) 150; N. Sakai, Z. Phys. **C11** (1981) 153; E. Witten, Nucl. Phys. **B188** (1981) 513; H.P. Nilles, Phys. Rep. **110** (1984) 1; H.E. Haber and G.L. Kane, Phys. Rep. **117** (1985) 75; M.F. Sohnius, Phys. Rep. **128** (1985) 39; J.F. Gunion and H.E. Haber, Nucl. Phys. **B272** (1986) 1 [Erratum-ibid. **B402** (1993) 567], Nucl. Phys. **B278** (1986) 449; A.B. Lahanas and D.V. Nanopoulos, Phys. Rep. **145** (1987) 1.
- [4] For reviews and further references, see: J.F. Gunion, H.E. Haber, G. Kane and S. Dawson, “*The Higgs Hunter’s Guide*”, Addison-Wesley, 1990; S.P. Martin, [hep-ph/9709356]; S. Dawson, [hep-ph/9712464]; M. Gomez-Bock, M. Mondragon, M. Mühlleitner, R. Noriega-Papaqui, I. Pedraza, M. Spira and P. M. Zerwas, J. Phys. Conf. Ser. **18** (2005) 74 [arXiv:hep-ph/0509077]; M. Gomez-Bock, M. Mondragon, M. Mühlleitner, M. Spira and P. M. Zerwas, [arXiv:0712.2419 [hep-ph]]; A. Djouadi, Phys. Rept. **459** (2008) 1 [hep-ph/0503173].
- [5] P. Fayet, Nucl. Phys. **B90** (1975) 104; R. Barbieri, S. Ferrara, C. A. Savoy, Phys. Lett. **B119** (1982) 343; M. Dine, W. Fischler, M. Srednicki, Phys. Lett. **B104** (1981) 199; H. P. Nilles, M. Srednicki, D. Wyler, Phys. Lett. **B120** (1983) 346; J. M. Frere, D. R. T. Jones, S. Raby, Nucl. Phys. **B222** (1983) 11; J. P. Derendinger, C. A. Savoy, Nucl. Phys. **B237** (1984) 307; J. R. Ellis, J. F. Gunion, H. E. Haber, L. Roszkowski, F. Zwirner, Phys. Rev. **D39** (1989) 844; M. Drees, Int. J. Mod. Phys. **A4** (1989) 3635; U. Ellwanger, M. Rausch de Traubenberg, C. A. Savoy, Phys. Lett. **B315** (1993) 331 [hep-ph/9307322], Z. Phys. **C67** (1995) 665 [hep-ph/9502206], Nucl. Phys. **B492** (1997) 21 [hep-ph/9611251]; T. Elliott, S. F. King, P. L. White, Phys. Lett. **B351** (1995) 213 [hep-ph/9406303]; S. F. King, P. L. White, Phys. Rev. **D52** (1995) 4183 [hep-ph/9505326]; F. Franke, H. Fraas, Int. J. Mod. Phys. **A12** (1997) 479 [hep-ph/9512366]; M. Maniatis, Int. J. Mod. Phys. **A25** (2010) 3505 [arXiv:0906.0777 [hep-ph]]; U. Ellwanger, C. Hugonie, A. M. Teixeira, Phys. Rept. **496** (2010) 1 [arXiv:0910.1785 [hep-ph]].
- [6] J.E. Kim and H.P. Nilles, Phys. Lett. **B138** (1984) 150.
- [7] M. Bastero-Gil, C. Hugonie, S. F. King, D. P. Roy and S. Vempati, Phys. Lett. B **489**, 359 (2000) [hep-ph/0006198]; A. Delgado, C. Kolda, J. P. Olson and A. de la Puente, Phys. Rev. Lett. **105**, 091802 (2010) [arXiv:1005.1282 [hep-ph]]; U. Ellwanger, G. Espitalier-Noel and C. Hugonie, JHEP **1109** (2011) 105 [arXiv:1107.2472 [hep-ph]]; G. G. Ross and K. Schmidt-Hoberg, arXiv:1108.1284 [hep-ph].
- [8] S. F. King, M. Mühlleitner and R. Nevzorov, Nucl. Phys. B **860** (2012) 207 [arXiv:1201.2671 [hep-ph]].
- [9] L. J. Hall, D. Pinner and J. T. Ruderman, JHEP **1204** (2012) 131 [arXiv:1112.2703 [hep-ph]].
- [10] U. Ellwanger, Phys. Lett. B **698** (2011) 293 [arXiv:1012.1201 [hep-ph]]; U. Ellwanger, JHEP **1203** (2012) 044 [arXiv:1112.3548 [hep-ph]]; A. Arvanitaki and G. Villadoro, JHEP **1202** (2012) 144 [arXiv:1112.4835 [hep-ph]].
- [11] E. Accomando *et al.*, hep-ph/0608079.

- [12] A. Pilaftsis, Phys. Lett. B **435** (1998) 88 [hep-ph/9805373]; D. A. Demir, Phys. Rev. D **60** (1999) 055006 [hep-ph/9901389]; A. Pilaftsis and C. E. M. Wagner, Nucl. Phys. B **553** (1999) 3 [hep-ph/9902371]; S. Y. Choi, M. Drees and J. S. Lee, Phys. Lett. B **481** (2000) 57 [hep-ph/0002287]; M. S. Carena, J. R. Ellis, A. Pilaftsis and C. E. M. Wagner, Nucl. Phys. B **586** (2000) 92 [hep-ph/0003180]; T. Ibrahim and P. Nath, Phys. Rev. D **63** (2001) 035009 [hep-ph/0008237] and Phys. Rev. D **66** (2002) 015005 [hep-ph/0204092]; S. Heinemeyer, Eur. Phys. J. C **22** (2001) 521 [hep-ph/0108059]; M. S. Carena, J. R. Ellis, A. Pilaftsis and C. E. M. Wagner, Nucl. Phys. B **625** (2002) 345 [hep-ph/0111245]; S. W. Ham, S. K. Oh, E. J. Yoo, C. M. Kim and D. Son, Phys. Rev. D **68** (2003) 055003 [hep-ph/0205244]; M. Frank, S. Heinemeyer, W. Hollik and G. Weiglein, hep-ph/0212037; S. Heinemeyer, Int. J. Mod. Phys. A **21** (2006) 2659 [hep-ph/0407244]; S. Heinemeyer, W. Hollik, H. Rzehak and G. Weiglein, Phys. Lett. B **652** (2007) 300 [arXiv:0705.0746 [hep-ph]].
- [13] M. Frank, T. Hahn, S. Heinemeyer, W. Hollik, H. Rzehak, G. Weiglein, JHEP **0702** (2007) 047 [hep-ph/0611326].
- [14] E. Christova, H. Eberl, W. Majerotto and S. Kraml, Nucl. Phys. B **639** (2002) 263 [Erratum-ibid. B **647** (2002) 359] [hep-ph/0205227]; E. Christova, H. Eberl, W. Majerotto and S. Kraml, JHEP **0212** (2002) 021 [hep-ph/0211063]; . Khater and P. Osland, Nucl. Phys. B **661** (2003) 209 [hep-ph/0302004]; S. Y. Choi, J. Kalinowski, Y. Liao and P. M. Zerwas, Eur. Phys. J. C **40** (2005) 555 [hep-ph/0407347]; K. E. Williams and G. Weiglein, Phys. Lett. B **660** (2008) 217 [arXiv:0710.5320 [hep-ph]]; K. E. Williams, H. Rzehak and G. Weiglein, Eur. Phys. J. C **71** (2011) 1669 [arXiv:1103.1335 [hep-ph]].
- [15] M. S. Carena, J. R. Ellis, A. Pilaftsis and C. E. M. Wagner, Phys. Lett. B **495** (2000) 155 [hep-ph/0009212]; M. S. Carena, J. R. Ellis, S. Mrenna, A. Pilaftsis and C. E. M. Wagner, Nucl. Phys. B **659** (2003) 145 [hep-ph/0211467]; A. Dedes and S. Moretti, Phys. Rev. Lett. **84** (2000) 22 [hep-ph/9908516]; A. Dedes and S. Moretti, Nucl. Phys. B **576** (2000) 29 [hep-ph/9909418]; S. Y. Choi and J. S. Lee, Phys. Rev. D **61** (2000) 115002 [hep-ph/9910557]; S. Y. Choi, K. Hagiwara and J. S. Lee, Phys. Lett. B **529** (2002) 212 [hep-ph/0110138]; A. Arhrib, D. K. Ghosh and O. C. W. Kong, Phys. Lett. B **537** (2002) 217 [hep-ph/0112039]; B. E. Cox, J. R. Forshaw, J. S. Lee, J. Monk and A. Pilaftsis, Phys. Rev. D **68** (2003) 075004 [hep-ph/0303206]; A. G. Akeroyd, Phys. Rev. D **68** (2003) 077701 [hep-ph/0306045]; F. Borzumati, J. S. Lee and W. Y. Song, Phys. Lett. B **595** (2004) 347 [hep-ph/0401024]; V. A. Khoze, A. D. Martin and M. G. Ryskin, Eur. Phys. J. C **34** (2004) 327 [hep-ph/0401078]; J. R. Ellis, J. S. Lee and A. Pilaftsis, Phys. Rev. D **70** (2004) 075010 [hep-ph/0404167]; D. K. Ghosh, R. M. Godbole and D. P. Roy, Phys. Lett. B **628** (2005) 131 [hep-ph/0412193]; D. K. Ghosh and S. Moretti, Eur. Phys. J. C **42** (2005) 341 [hep-ph/0412365]; J. R. Ellis, J. S. Lee and A. Pilaftsis, Phys. Rev. D **71** (2005) 075007 [hep-ph/0502251].
- [16] J. C. Romao, Phys. Lett. B **173** (1986) 309.
- [17] B. C. Regan, E. D. Commins, C. J. Schmidt and D. DeMille, Phys. Rev. Lett. **88** (2002) 071805; C. A. Baker *et al.*, Phys. Rev. Lett. **97** (2006) 131801 [hep-ex/0602020]; W. C. Griffith *et al.*, Phys. Rev. Lett. **102** (2009) 101601.

- [18] M. Matsuda and M. Tanimoto, Phys. Rev. D **52** (1995) 3100 [hep-ph/9504260]; N. Haba, Prog. Theor. Phys. **97** (1997) 301 [hep-ph/9608357]; T. Ibrahim and P. Nath, Phys. Rev. D **58** (1998) 111301 [Erratum-ibid. D **60** (1999) 099902] [hep-ph/9807501]; J. R. Ellis, J. S. Lee and A. Pilaftsis, JHEP **0810** (2008) 049 [arXiv:0808.1819 [hep-ph]]; M. Boz, Mod. Phys. Lett. A **21** (2006) 243 [hep-ph/0511072].
- [19] K. Cheung, T. -J. Hou, J. S. Lee and E. Senaha, Phys. Rev. D **84** (2011) 015002 [arXiv:1102.5679 [hep-ph]].
- [20] R. Garisto, Phys. Rev. D **49** (1994) 4820 [hep-ph/9311249].
- [21] S. W. Ham, J. Kim, S. K. Oh and D. Son, Phys. Rev. D **64** (2001) 035007 [hep-ph/0104144]; S. W. Ham, S. H. Kim, S. K. OH and D. Son, Phys. Rev. D **76** (2007) 115013 [arXiv:0708.2755 [hep-ph]].
- [22] S. W. Ham, S. K. Oh and D. Son, Phys. Rev. D **65** (2002) 075004 [hep-ph/0110052]; S. W. Ham, Y. S. Jeong and S. K. Oh, hep-ph/0308264.
- [23] K. Funakubo and S. Tao, Prog. Theor. Phys. **113** (2005) 821 [hep-ph/0409294].
- [24] K. Cheung, T. -J. Hou, J. S. Lee and E. Senaha, Phys. Rev. D **82** (2010) 075007 [arXiv:1006.1458 [hep-ph]].
- [25] U. Ellwanger, Phys. Lett. **B303** (1993) 271 [hep-ph/9302224]; T. Elliott, S. F. King, P. L. White, Phys. Lett. **B305** (1993) 71 [hep-ph/9302202], Phys. Lett. **B314** (1993) 56 [hep-ph/9305282], Phys. Rev. **D49** (1994) 2435 [hep-ph/9308309]; P. N. Pandita, Z. Phys. **C59** (1993) 575, Phys. Lett. **B318** (1993) 338; U. Ellwanger, C. Hugonie, Phys. Lett. **B623** (2005) 93 [hep-ph/0504269]; G. Degrassi, P. Slavich, Nucl. Phys. **B825** (2010) 119 [arXiv:0907.4682 [hep-ph]]; F. Staub, W. Porod, B. Herrmann, JHEP **1010** (2010) 040 [arXiv:1007.4049 [hep-ph]].
- [26] K. Ender, T. Graf, M. Muhlleitner and H. Rzehak, Phys. Rev. D **85** (2012) 075024 [arXiv:1111.4952 [hep-ph]].
- [27] R. Barate *et al.* [LEP Working Group for Higgs boson searches], Phys. Lett. B **565** (2003) 61 [hep-ex/0306033]; S. Schael *et al.* [ALEPH and DELPHI and L3 and OPAL Collaborations], Eur. Phys. J. C **47** (2006) 547 [hep-ex/0602042].
- [28] [TEVNP (Tevatron New Phenomena and Higgs Working Group) and CDF and D0 Collaborations], arXiv:1203.3774 [hep-ex].
- [29] M. Kobayashi and T. Maskawa, Prog. Theor. Phys. **49** (1973) 652.
- [30] A. Denner, Fortsch. Phys. **41** (1993) 307 [arXiv:0709.1075 [hep-ph]].
- [31] A. Brignole, Phys. Lett. B **281** (1992) 284, P. H. Chankowski, S. Pokorski, J. Rosiek; Phys. Lett. **B286** (1992) 307, Nucl. Phys. **B423** (1994) 437 [hep-ph/9303309]; A. Dabelstein, Z. Phys. **C67** (1995) 495 [hep-ph/9409375], Nucl. Phys. **B456** (1995) 25 [hep-ph/9503443]; A. Freitas and D. Stockinger, Phys. Rev. D **66** (2002) 095014 [hep-ph/0205281].

- [32] M. Frank, Berlin, Germany: RHOMBOS-Verl. (2003) 148 p.
- [33] W. Hollik, E. Kraus, M. Roth, C. Rupp, K. Sibold and D. Stockinger, Nucl. Phys. B **639** (2002) 3 [hep-ph/0204350].
- [34] J. Kublbeck, M. Bohm, A. Denner, Comput. Phys. Commun. **60** (1990) 165; T. Hahn, Comput. Phys. Commun. **140** (2001) 418 [hep-ph/0012260]; T. Hahn, C. Schappacher, Comput. Phys. Commun. **143** (2002) 54 [hep-ph/0105349].
- [35] F. Staub, [arXiv:0806.0538 [hep-ph]], Comput. Phys. Commun. **181** (2010) 1077 [arXiv:0909.2863 [hep-ph]], Comput. Phys. Commun. **182** (2011) 808 [arXiv:1002.0840 [hep-ph]].
- [36] T. Hahn, M. Perez-Victoria, Comput. Phys. Commun. **118** (1999) 153 [hep-ph/9807565]; T. Hahn, Comput. Phys. Commun. **178** (2008) 217 [hep-ph/0611273].
- [37] F. del Aguila, A. Culatti, R. Munoz Tapia, M. Perez-Victoria, Nucl. Phys. **B537** (1999) 561 [hep-ph/9806451].
- [38] P. Z. Skands, B. C. Allanach, H. Baer, C. Balazs, G. Belanger, F. Boudjema, A. Djouadi, R. Godbole *et al.*, JHEP **0407** (2004) 036 [hep-ph/0311123]; B. C. Allanach, C. Balazs, G. Belanger, M. Bernhardt, F. Boudjema, D. Choudhury, K. Desch, U. Ellwanger *et al.*, Comput. Phys. Commun. **180** (2009) 8 [arXiv:0801.0045 [hep-ph]]; F. Mahmoudi, S. Heinemeyer, A. Arbey, A. Bharucha, T. Goto, T. Hahn, U. Haisch, S. Kraml *et al.*, [arXiv:1008.0762 [hep-ph]].
- [39] U. Ellwanger, J.F. Gunion and C. Hugonie, JHEP **0502** (2005) 066; U. Ellwanger and C. Hugonie, Comput. Phys. Commun. **175** (2006) 290; U. Ellwanger and C. Hugonie, Comput. Phys. Commun. **177** (2007) 399;
(see also <http://www.th.u-psud.fr/NMHDECAY/nmssmtools.html>).
- [40] K. Nakamura *et al.* (Particle Data Group), J. Phys. **G37** (2010) 075021 and 2011 partial update for the 2012 edition.
- [41] P. Bechtle, O. Brein, S. Heinemeyer, G. Weiglein and K. E. Williams, Comput. Phys. Commun. **181** (2010) 138 [arXiv:0811.4169 [hep-ph]]; P. Bechtle, O. Brein, S. Heinemeyer, G. Weiglein and K. E. Williams, Comput. Phys. Commun. **182** (2011) 2605 [arXiv:1102.1898 [hep-ph]].
- [42] M. Spira, “HIGLU: A Program for the Calculation of the Total Higgs Production Cross-Section at Hadron Colliders via Gluon Fusion including QCD Corrections,” [hep-ph/9510347].
- [43] URL: <http://people.web.psi.ch/spira/proglist.html>
- [44] W. Beenakker, S. Dittmaier, M. Kramer, B. Plumper, M. Spira and P. M. Zerwas, Phys. Rev. Lett. **87** (2001) 201805 [hep-ph/0107081]; Nucl. Phys. B **653** (2003) 151 [hep-ph/0211352]; L. Reina and S. Dawson, Phys. Rev. Lett. **87** (2001) 201804, arXiv:hep-ph/0107101; S. Dawson, L. H. Orr, L. Reina and D. Wackerth, Phys. Rev. D **67**, 071503 (2003) [hep-ph/0211438].
- [45] S. Dittmaier *et al.* [LHC Higgs Cross Section Working Group Collaboration], arXiv:1101.0593 [hep-ph];
URL: <https://twiki.cern.ch/twiki/bin/view/LHCPhysics/CrossSections>

- [46] A. Djouadi, M. Spira and P.M. Zerwas, Phys. Lett. B **264** (1991) 440 and Z. Phys. C **70** (1996) 427; M. Spira *et al.*, Nucl. Phys. B **453** (1995) 17; A. Djouadi, J. Kalinowski and M. Spira, Comput. Phys. Commun. **108** (1998) 56; A. Djouadi, J. Kalinowski, M. Muhlleitner and M. Spira in J. M. Butterworth *et al.*, arXiv:1003.1643 [hep-ph].
- [47] A. Djouadi, M. M. Muhlleitner and M. Spira, Acta Phys. Polon. **B38** (2007) 635 [hep-ph/0609292].
- [48] G. Aad *et al.* [ATLAS Collaboration], Phys. Lett. B **701** (2011) 186 [arXiv:1102.5290 [hep-ex]]; Phys. Lett. B **701** (2011) 398 [arXiv:1103.4344 [hep-ex]]; G. Aad *et al.* [ATLAS Collaboration], Phys. Lett. B **710** (2012) 67 [arXiv:1109.6572 [hep-ex]]. G. Aad *et al.* [ATLAS Collaboration], Phys. Rev. D **85** (2012) 012006 [arXiv:1109.6606 [hep-ex]]; G. Aad *et al.* [Atlas Collaboration], JHEP **1111** (2011) 099 [arXiv:1110.2299 [hep-ex]]; G. Aad *et al.* [ATLAS Collaboration], Phys. Rev. Lett. **108** (2012) 181802 [arXiv:1112.3832 [hep-ex]].
- [49] S. Chatrchyan *et al.* [CMS Collaboration], Phys. Rev. Lett. **107** (2011) 221804 [arXiv:1109.2352 [hep-ex]]; The CMS Collaboration, CMS-PAS-SUS-11-002, CMS-PAS-SUS-11-005, CMS-PAS-SUS-11-010, CMS-PAS-SUS-11-016.
- [50] G. Belanger, F. Boudjema, A. Pukhov and A. Semenov, Comput. Phys. Commun. **149** (2002) 103 [hep-ph/0112278], Comput. Phys. Commun. **174** (2006) 577 [hep-ph/0405253] and Comput. Phys. Commun. **180** (2009) 747 [arXiv:0803.2360 [hep-ph]]; G. Belanger *et al.*, Comput. Phys. Commun. **182** (2011) 842 [arXiv:1004.1092 [hep-ph]].
- [51] G. Aad *et al.* [ATLAS Collaboration], Phys. Lett. B **701** (2011) 1 [arXiv:1103.1984 [hep-ex]]; G. Aad *et al.* [ATLAS Collaboration], [arXiv:1203.6193 [hep-ex]]; G. Aad *et al.* [ATLAS Collaboration], arXiv:1204.6736 [hep-ex].
- [52] S. Chatrchyan *et al.* [CMS Collaboration], arXiv:1205.3933 [hep-ex]; The CMS Collaboration, CMS-PAS-SUS-11-027, CMS-PAS-SUS-11-028.